Light and Dark Active Phosphodiesterase Regulation in Salamander Rods

W. H. COBBS

From the Department of Biochemistry and Biophysics, University of Pennsylvania School of Medicine, Philadelphia, Pennsylvania 19104

ABSTRACT We studied the activation of 3′,5′-cyclic guanosine monophosphate (cGMP) phosphodiesterase (PDE) by using a cell-permeant enzyme inhibitor. Rods of *Ambystoma tigrinum* held in a suction electrode were jumped into a stream of 3-isobutyl-1-methylxanthine (IBMX), 0.01–1 mM. Initial transient light-sensitive currents fit the notion that dark and light-activated forms of PDE contributed independently to metabolic activity and were equivalently inhibited by IBMX (apparent K_i 30 μm). Inhibition developed within 50 ms, producing a step decrease of enzyme velocity, which could be offset by activation with flashes or steps of light. The dark PDE activity was equivalent to light activation of enzyme by 1,000 isomerization $rod^{-1}s^{-1}$, sufficient to hydrolyze the free cGMP pool ($1/e$) in 0.6 s. Steady light activated PDE in linear proportion to isomerization rate, the range from darkness to current saturation amounting to a 10-fold increase. The conditions for simultaneous onset of inhibitor and illumination to produce no net change of membrane current defined the apparent lifetime of light-activated PDE, $T_{PDE^*} = 0.9$ s, which was independent of both background illumination and current over the range $0–3 \times 10^5$ isomerization s^{-1}, from 50 to 0 pA. Adaptation was a function of current rather than isomerization: jumps with different proportions of IBMX concentration to steady light intensity produced equal currents, and followed the same course of adaptation in maintained light, despite a 10-fold difference of illumination. Judged from the delay between IBMX- and light-induced currents, the dominant feedback regulatory site comes after PDE on the signal path. The dark active PDE affects the hydrolytic flux and cytoplasmic diffusion of cGMP, as well as the proportional range of the cGMP activity signal in response to light.

INTRODUCTION

This work examines three aspects of signaling by visual cells: the regulation of the quiescent dark state, the deactivating step after excitation, and the feedback control of dynamic range in light adaptation. The concerns are common to receptor pathways coupled by guanosine triphosphate (GTP)-binding signal proteins.

Address reprint requests to Dr. W. H. Cobbs, Department of Biochemistry and Biophysics, University of Pennsylvania School of Medicine, 6th Floor Richards Building, 37th and Hamilton Walk, Philadelphia, PA 19104-6089.

J. GEN. PHYSIOL. © The Rockefeller University Press · 0022-1295/91/09/0575/40 $2.00
Volume 98 September 1991 575–614

The elements connecting isomerization of the visual pigment to modulation of the rod light-sensitive membrane current are arranged as an enzyme cascade, which passes signal rather than substance from stage to stage. The kinetic properties of this pathway determine the quantum sensitivity and light adaptation characteristics of photoreceptors.

In vertebrates, the hydrolytic enzyme 3′-5′:cyclic guanosine monophosphate (cGMP) phosphodiesterase (PDE) occupies a central position in the visual cascade. PDE interacts with both the α subunit of GTP-binding protein (transducin), activated by photoisomerized rhodopsin, and with the substrate cGMP, synthesized via guanylyl cyclase (GCy). Free cGMP directly activates conducting states of the light-sensitive channel by cooperative ligand binding. Together with guanylyl cyclase PDE controls cGMP; via cGMP it governs the light-sensitive conductance and thereby both Na^+ and Ca^{2+} influx through the plasma membrane. The loss of cGMP by hydrolysis is redressed by local synthesis, so that the reaction velocities of PDE and guanylyl cyclase sum in the free cGMP pool of the visual cell outer segment. This constraint supplies a tool useful to probe system control.

The utility of the visual cell as a photon detector depends on the stability of the rod membrane current; hence the control of PDE activity in darkness is a basic concern. The rate of enzyme deactivation after an isomerization affects both the light sensitivity and signal bandwidth of the cell. The rates of deactivation of GTP-binding protein inferred from in vitro assays of GTP-ase rates ($< 1\ s^{-1}$) are slow compared to the duration of single photon responses (Sitaramayya et al., 1988). For this reason, the measurement of the activated PDE lifetime in the functioning cell is of particular interest.

Several observations suggest that an important feedback mechanism acts near the site of an isomerization. A flash stimulus reduces light sensitivity, but only after a delay; the desensitization produced by focal illumination of a rod outer segment remains localized, like the single photon current. An important clue to the mechanism is that conditions that impede Ca^{2+} transport across the outer segment plasma membrane strongly curtail light adaptation (Matthews et al., 1988; Nakatani and Yau, 1988*b*). The connection of Ca^{2+} to cGMP metabolism remains uncertain, but suppression of guanylyl cyclase activation by cytoplasmic Ca^{2+} is thought to be important (Hodgkin and Nunn, 1988; Koch and Stryer, 1988). A calcium-independent component of light adaptation is also proposed (Kawamura and Murakami, 1989; Nichol and Bownds, 1989; Rispoli and Detwiler, 1989).

The goals were limited to estimates of the apparent activation and decay rates of PDE in isolated rods over the range of light reception. Perturbations of PDE activation with light were made either with membrane current free to move in response to change of PDE velocity, or fixed through the use of a cell-permeant PDE inhibitor. Thus we measured rates with outer segment cytoplasmic cGMP activity and Ca^{2+} balance held constant, interrupting a suspected current-mediated feedback. The inhibitor 3-isobutyl-1-methylxanthine (IBMX) is uncharged, lipid-soluble, and inert to metabolic transformation, so its free cytoplasmic activity should follow a simple equilibrium with the external solution.

Preliminary results have been presented (Cobbs, 1989).

METHODS

Animals and Cell Isolation

Under infrared visualization dark-adapted larval salamanders (150 g, Lowrance Waterdogs, Tulsa, OK) were instantly decapitated and spinally pithed. The globes were hemisected and from the freed retina single cells liberated by freehand mincing with a razor blade. Aliquots suspended in 5 mM glucose 4-(2-hydroxyethl-1-piperazine ethane sulfonate (HEPES) Ringer's were kept on ice and injected into the experimental chamber as needed. Cells were taken for recording based on criteria of at least 25-pA dark current and active light adaptation, as verified by recovery of membrane current in steady light of initially just-saturating intensity. Data were discarded if dark current declined from the initial value by > 20% during the course of observations.

Optics and Stimulus

The apparatus constructed in the Department of Biochemistry and Biophysics followed closely a previous plan (Cobbs and Pugh, 1987). An inverted microscope (model ICM405, Carl Zeiss, Inc., Thornwood, NY) with an infrared video camera (SC-67M Dage-MTI, Inc., Michigan City, IN) received the experimental chamber. Optical access from above allowed illumination from four coaxial beams imaged through a model UDT 20 × 0.57 (Carl Zeiss, Inc.) numerical aperture objective functioning as condenser. The coaxial beams provided infrared field illumination, and three independently controlled visible wavelength stimuli derived from a grating monochromator (Schoeffel), a 100-J Xe discharge tube (EG&G Electro-Optics, Salem, MA), or a filtered 50-W tungsten halogen filament. The visible light stimulus was defined by a movable slit; infrared could be shone through the slit to position and focus the stimulus image without exposing the cell to visible light. The intensity of the grating monochromator beam, excited by a 50-W tungsten halogen filament supplied from a stabilized direct current (DC) power supply, was measured directly at the object plane. The reference photodiode was a U.S. National Bureau of Standards–traceable unit of calibrated spectral sensitivity (PIN-10DFP, UDT Co., Hawthorne, CA). The flux of the unattenuated 520-nm beam at the specimen was 3.05×10^6 quanta $\mu m^{-2} s^{-1}$. This light was linearly polarized with the axis at 45° to a normal to the photoreceptor disks. Other stimuli were calibrated from the monochromatic beam by matched comparison of photoreceptor responses in the linear response range. Bright-field fluorite objectives (20, 40, and 63×) were used throughout. Video recordings or monitor photographs were taken of individual cells to assess their optical collecting areas; in their absence the mean value of 114 μm^2 was used (Cobbs and Pugh, 1987). This value is substantially larger-than the 20-μm^2 value adopted by Hodgkin and Nunn (1988). The reason for the discrepancy is not known. Light stimulus intensities in this paper are generally reported as isomerizations per rod, abbreviated "isom." The entire optical train, Huxley micromanipulators, suction electrode hydraulic drive, and headstages were mounted on a vibration isolation table (Newport Corp., Fountain Valley, CA). The recording area of the table was enclosed by a freestanding floor-mounted light-proof Faraday cage.

Recording

The recording chamber was connected to signal ground via Ringer's and KCl agar bridges and a saturated KCl|AgCl|Ag junction with a path resistance of 7 kΩ. The suction electrode was mounted in a polycarbonate holder (E. W. Wright, Guilford, CT). A Luer fitting joined the holder to a truncated glass tuberculin syringe body containing a saturated KCl|AgCl|Ag junction sealed over with epoxy cement; this end fit the BNC connector of the 1 GΩ amplifier headstage. A tetrafluorethylene (TFE) frit (Alltech Associates, Inc., Deerfield, IL) plugged with

Ringer's agar formed the Ringer's|KCl junction. A sidearm from the electrode holder was connected by 0.25-mm bore Tefzel HPLC tubing filled with silicon oil to a syringe micrometer drive or alternately via a T-valve (Hamilton Co., Reno, NV) to an adjustable open U-tube.

The output of a model 8900 clamp amplifier (Dagan Corp., Minneapolis, MN) operated in voltage clamp mode at 1000 Hz bandwidth was conditioned by an eight-pole Bessel Filter (Frequency Devices Inc., Haverill, MA) usually set to 20 Hz and +20 dB gain. Signals were digitized at either 100 Hz or 500 Hz rates via an analog/digital (A/D) converter (Scientific Solutions, Inc., Solon, OH) controlled by a Z8 microprocessor with custom interface and software package (Dr. Roy Furman, University of Pennsylvania, Philadelphia, PA) and stored as transients of 2.5, 5, 10, or 20 s duration on the hard disk of a Bentley 12 MHz 80286 IBM AT-compatible computer. In some experiments a second signal pathway substantially duplicating the first was used to measure junction currents. The time and the status of amplifier gain settings, optical stimuli and solutions were recorded automatically with each transient. An electronic shutter gating the monochromator channel, the Xe flash, and the jumping stage (see below) were all computer driven using programmable asynchronous timers (Scientific Solutions, Inc.). Continuous data were also displayed on a strip chart and recorded digitally on VCR tape (SONY Unitrade). The relative timing of light stimuli, jumping stage motion, and recorded membrane current transients was verified by propagating analogues of each through the membrane current signal path.

Chamber and Solution Flow

The experimental chamber (Fig. 1 *A*, *inset*) was constructed of Lexan polycarbonate with a V-shaped notch bridged on either side by a coverslip, the wide mouth of the V presenting a free meniscus for insertion to the suction electrode and access by a sucker which aspirated effluent Ringer's. The coverslips were separated by 3 mm and enclosed a fluid volume of 100 μl. Solutions flowed into the chamber at the apex of the V, where three channels of 1-mm^2 cross-section milled in the plastic converged. The center channel was filled with Ringer's agar to form the ground bridge. The channels on either side met at 90° and continued for 2 mm as a common straight passage of 1.4-mm width. Here the two streams continued side by side in laminar flow. For recording, the cell held in the suction electrode was thrust into the common channel ~200 μm downstream from the juncture and 100 μm above the passage floor.

All solutions flowed by gravity down a 0.5-m drop at rates determined by pediatric intravenous anesthesia valves (Multiflow; Abbott Laboratories, Chicago, IL). One channel was always set to control Ringer's. The second channel was connected to a two-way solenoid-actuated valve of 7 μl internal volume (Lee Co., Westbrook, CT) which in turn was fed on either side by a solenoid-actuated valve (Lee Co.), which could be set either to drain or to feed the center valve. Finally, each side valve could receive one of six solutions (total 12) from a manually operated multiway valve (Rheodyne Inc., Cotati, CA). In this way, either of two previously primed solutions could be presented to the experimental side of the laminar flow passage with a lag time of 5 s; the dead volume of the connecting tubings could be washed through the side valves to prime a new selection while another flowed in the test channel. Surfaces contacting Ringer's were either fluoropolymer (Teflon) or polyethylene except as noted.

The temperature of the chamber was maintained at ~ 18°C by chilling the control Ringer's as the tubing passed through an ice bath. The experimental solution flowed through a 5-cm segment of 0.25-mm bore polyethylene tubing threaded concentrically through the wall of a 1-mm bore silicone rubber segment of the control solution tubing. In this way temperature control was achieved at minimal cost of additional dead space, the two channels were equilibrated to the same temperature, and any thermal contamination from the solenoid valves

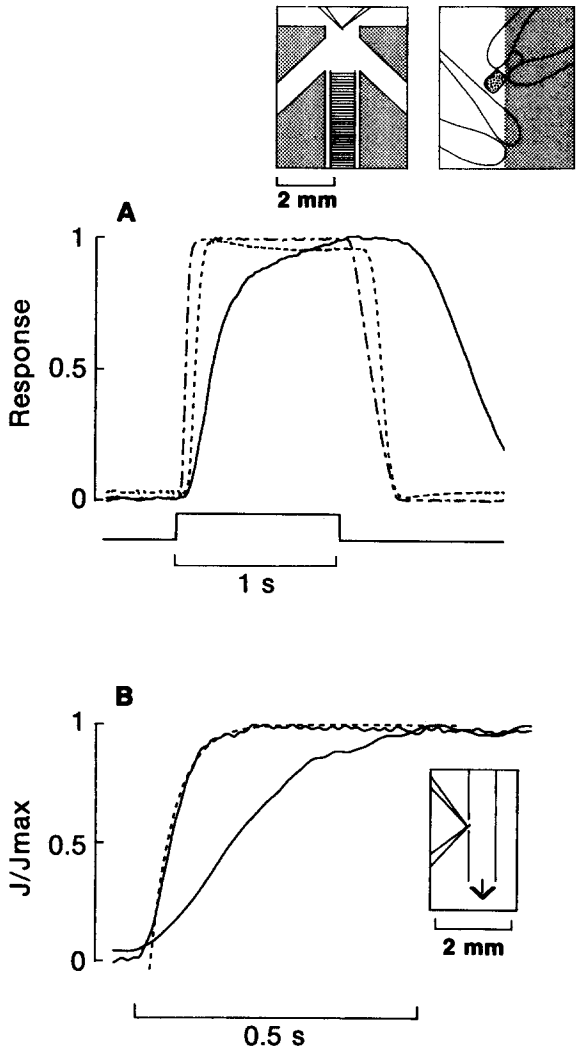

FIGURE 1. Onset of IBMX and IBMX-induced current. (*A*) Jumping stage, timing of rod membrane current in relation to chamber motion and solution composition change. Photocell current (interrupted trace) was proportional to chamber displacement. Junction current (dashed trace) was collected by a voltage-clamped probe electrode poised ~50 μm upstream from the rod, at the interface between experimental and control solutions (*inset right*). The solid trace is IBMX-induced rod membrane current collected by a suction electrode, pipette-inward current plotted up, under duplicate conditions of solution flow. All three responses are scaled to unity for comparison. The timing trace at bottom marks trigger of jump onset and return. The mean velocity of solution flow was 1 mm s^{-1}; experimental solution, Ringer's IBMX 156 μM, diluted by 3% with ion-free water to produce a junction current. Recording bandwidth 20 Hz, cell #1. (*Inset left*) Configuration of flow channels, pipette electrodes, and ground pathway. (*Inset right*) Tracing from video record showing position of suction electrode pipette, rod cell, junction current probe electrode, and flow boundary. (*B*) Side-hole flow tube, timing of IBMX-induced current in relation to junction current. Uppermost solid trace, probe electrode junction current; dashed trace, exponential curve with $T_{0.5}$ 20 ms; lower solid trace, rod suction electrode light-sensitive current, mean of four trials, light-insensitive current subtracted. The junction current transition approximated the cell membrane time constant, but the IBMX-induced current response was not substantially faster than in *A*. (*Inset*) The rod outer segment extended from a suction electrode into the side hole of a capillary with flowing inhibitor solution, which gushed out when the capillary drain was stopped by an automated valve (not shown). The outer segment and a voltage-clamped probe electrode as in Panel A were placed alternately in the same position. Experimental solution, Ringer's 200 μM IBMX diluted 5% with ion-free water, bath solution Ringer's. Recording bandwidth 50 Hz. Cell 2.

was obviated. Temperature was measured with a 0.64-mm diam thermocouple probe (IT-18, Sensotec Inc., Columbus, OH) thrust into the recording position.

Fast changes of solution ("jumps") were produced by shifting the entire chamber with respect to the suction electrode to move the interface between the two flowing solutions past the cell (Fig. 1). The chamber was translated parallel to the microscope object plane and normal to the direction of solution flow by a hydraulic slave cylinder plunger driven by a remote solenoid-actuated master (Hodgkin et al., 1985). The jump excursion was adjusted to 0.2 mm. Displacement was monitored by a photocell receiving the stimulus beam interrupted by an opaque tape vane attached to the chamber. The transition, after a lag period, was nearly linear and half-complete within 50 ms. The motion of the interface between solutions from channels 1 and 2 was investigated using junction currents produced by diluting one solution by 3%. A 10 MΩ Ringer-filled pipette was introduced into the position of cell recording. When flow velocities exceeded 1 mm s^{-1} (recording condition), the transition of the junction current lagged the chamber motion by some 30 ms but occupied about the same elapsed time. At lower flow velocities the transition slowed markedly, presumably because a surface boundary layer adhered to the pipette.

Late in the investigation a capillary flow tube with a side hole aperture and an automated exit valve was substituted for the bilaminar flow pathway and jumping motion. This arrangement produced a faster change of composition at the outer segment, $T_{1/2}$ 20 ms (Fig. 1 *B*).

Solutions

The composition of the Ringer's was (in millimolar) NaCl 110, KCl 2.5, $MgCl_2$ 1.6, $CaCl_2$ 1.0, HEPES-free acid 10, NaEGTA 0.1, pH 7.50, with NaOH. Stock solutions of IBMX (Sigma Chemical Co., St. Louis, MO) 1.0–5.0 mM in ringer were diluted serially by twofold increments.

Data Reduction

Transients were filtered digitally by a 10-point moving average (20 Hz unless noted) before display. Linear detrending when necessary was accomplished either by subtraction of a control black trial or, in the case of short lived transients, from measurement of the baseline at the end of the sampling interval. Drift was usually <0.1 pA s^{-1}. Averaged transients were computed either on-line or assembled from individual transients buffered to disk. On-line screen displays of transients were dumped to a dot matrix printer; figures were recovered from disk records to an X–Y plotter. Curve-fitting analysis and least square regressions of derived parameters were computed using both commercial (Graftalk, DataEase International [Trumbull, CT]; Lotus 1-2-3, Lotus Development Co. [Cambridge, MA]) and custom software.

THEORY

Introduction

This section develops expressions for rod PDE in terms of stimulus light intensity, inhibitor concentration, and membrane current. Three constraints on cGMP simplify the task: (*a*) a hydrolytic rate in linear proportion to activity, (*b*) a synthetic rate independent of activity, and (*c*) a cGMP buffer strength negligible through the signal range of activity (Fig. 2). The relations of membrane current immediately following the stepwise application of an enzyme inhibitor or light stimulus will prove most useful. This interval begins with the constituents at their initial values and includes the lag phase of a feedback loop.

Symbols of enzyme reaction kinetics follow recommendations of the International Union of Biochemistry (Dixon, 1982); see Table I. Particular to this paper, enzyme

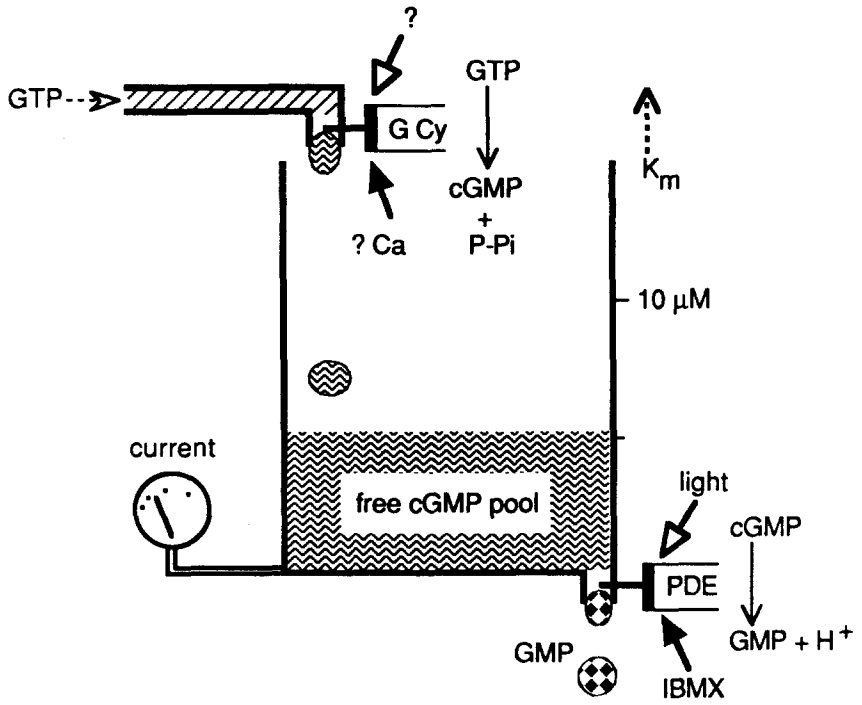

FIGURE 2. Kinetic concepts of the free cGMP pool. The hydraulic model portrays constraints on messengers within vertebrate photoreceptor outer segments. The free cGMP pool refers to the total free cGMP activity in outer segment cytoplasm. The GCy faucet feeds the pool independent of the free cGMP activity (pool level). The efflux via the drain controlled by cGMP PDE is nearly linear in cGMP activity, which lies far below the PDE Michaelis constant, $K_m \sim 1$ mM. The exponential lifetime of cGMP in the pool is given by the total content divided by the steady-state flow rate. Membrane current flowing through the cGMP-activated conductance provides a nonlinear gauge of cGMP activity, left side. Light activation can open the PDE drain, IBMX inhibition tends to close it. Elevated cytoplasmic Ca^{2+} is believed to close the GCy faucet, while other influences may open it.

TABLE I

Symbols for Enzyme Kinetic Quantities

Symbols	Units	Definition
s	M	Substrate activity
S	M	Substrate concentration
E_0	M	Enzyme concentration
v	s^{-1} M	Reaction velocity
V	s^{-1} M	Maximum velocity, saturating s
K_m	M	Michaelis constant, s: $v = V/2$
h	1	Hill cooperativity index
p	1	$1/h$ reciprocal Hill coefficient
k_{cat}	s^{-1}	Catalytic constant (turnover number)
k_{cat}/K_m	s^{-1} M^{-1}	Specificity constant
K_i	M	Inhibition constant

activity refers to the reaction velocity per physical quantity of enzyme under the standard condition of velocity saturation in substrate. This definition makes activity independent of the effect of a competitive inhibitor. Enzyme activation is taken as the ratio of observed enzyme activity to the activity expressed on maximal conversion to a catalytically competent form.

Dependence of Rod Current on Free cGMP

The rod light-sensitive channel is cooperatively gated by the cGMP ligand; other things being equal, the conductance serves as a nonlinear gauge of the activity level in the cGMP pool, shown at the left of Fig. 2. The majority carrier of inward current is Na^+, with a smaller proportion (20%) accounted by the permeant divalent blocking species, Ca^{2+} and Mg^{2+} (Nakatani and Yau, 1988*c*). Under physiologic conditions, current through the channel is nearly independent of voltage over the signal range of membrane potential; hence the outer segment may be approximated by the equivalent circuit element of a cGMP-regulated current source (Baylor and Nunn, 1986; Cobbs and Pugh, 1987).

Nakatani and Yau (1988*a*) studied the currents of broken toad rods dialyzed with cGMP in 100 μM IBMX. Current was a monotonic function of cGMP and distributed uniformly along the outer segment length; in the absence of GTP, light was without effect on the concentration dependence. Their observations obeyed the relation of Brown and Hill (1923), here rearranged to solve for s:

$$s^h = \frac{\frac{J}{J_{max}} K_{1/2}}{1 - \frac{J}{J_{max}}} \tag{1}$$

Rod current is J; J_{max}, the largest current at saturating (1 mM) cGMP; $h = 1.8$, the Hill coefficient; $K_{1/2} = 35$ μM. In salamander rods infused with cGMP under voltage clamp, $J_{max} > 1$ nA (Cobbs and Pugh, 1985). The approximation

$$\frac{s}{s_0} \approx \sqrt[h]{\frac{J}{J_0}} = j^p \tag{2}$$

where s_0 and J_0 refer to resting levels of cGMP and current in darkness, and $p = 1/h$ will be used throughout this article; for $J < 100$ pA, it falls short of the value from the more complete expression above by $<5\%$. The symbol j for the ratio J/J_0 simplifies typography. The possibility of false estimates of rod-free cGMP stemming from channel modulation by influences other than cGMP remains, although conclusive evidence is lacking.

Substrate Relations of cGMP Phosphodiesterase

The hydrolytic rate of PDE in vitro follows the Michaelis relation (Baehr et al., 1979):

$$v = \frac{V}{1 + \frac{K_m}{s}} \approx \frac{sV}{K_m} \tag{3}$$

The linear approximation is used throughout. For rods in darkness, s = 6 μM, 100 μM < K_m < 1000 μM, so the expected error lies between 6% and 0.6% (Nakatani and Yau, 1988*a*; Kawamura and Murakami, 1986*a*; Barkdoll et al., 1988). Observations of light-sensitive current suggest that the approximation remains valid in rods even when cGMP is substantially elevated by exogenous infusion (Cobbs and Pugh, 1985). The cGMP activity s is specified in preference to concentration S, which is dominated by cGMP bound to high affinity noncatalytic sites on PDE (Gillespie and Beavo, 1989).

In the absence of a cGMP source, s decays with an exponential time $T = K_m/V$ determined by PDE. The value of T sets a basic limit on the signal bandwidth impressed on s by PDE. Integration of Eq. 1 with initial boundary conditions t_0, s_0 yields the solution for s:

$$\ln\left(\frac{s}{s_0}\right) = \ln j^p = \frac{t - t_0}{T} \tag{4}$$

In the presence of a guanylyl cyclase source of cGMP, s and v may reach steady-state. If Eq. 1 is rearranged as $T = s/v$, T is seen to be the exponential turnover time of the exchangeable free cGMP pool at steady state.

Relations of GCy

For GCy the relation of enzyme velocity to substrate and product is quite different from the situation of PDE. Here cGMP is the product, GTP is the substrate, and both are displaced far from equilibrium. The presence of pyrophosphatase which splits inorganic pyrophosphate (P-P_i) makes the reaction effectively irreversible. Allosteric product inhibition by cGMP remains a logical possibility but lacks experimental support. The apparent association constant of GCy for GTP-Mg^{2+} is 7.9 × 10^{-4} M (Fleischman and Denisevich, 1979). In dialyzed broken toad rods, Kawamura and Murakami (1989) report a <20% increment in light sensitive current over the range from 1 to 6 mM GTP, with half-maximal current attained at 0.4 mM GTP. Throughout the remainder of this article GCy will be assumed to function at or near velocity saturation with respect to substrate. Hence both the velocity and activity of guanylyl cyclase may be symbolized by the single expression GCy. The cooperative regulation of GCy by Ca^{2+}, proposed by Hodgkin and Nunn (1988) and Koch and Stryer (1988), has is believed to be influenced by cGMP only at a distant site, via regulation of the light-sensitive conductance.

Kinetic Concepts of the Free cGMP Pool

When both GCy and PDE are active, the rate of change of free cGMP is given by the difference between synthesis and hydrolysis, corrected for the change of cGMP binding (Hodgkin and Nunn, 1988):

$$rv = \mathrm{GCy} - \frac{sV}{K_m} \tag{5}$$

Here GCy is GCy velocity, v, velocity of the composite reaction, r = ds/dS. If binding sites are negligible or saturated, then r = 1; the relation then gives the rate of free

cGMP change directly. The evidence for this assumption in rods has been reviewed (Nunn and Hodgkin, 1988). In brief, the noncatalytic sites of PDE are the major bound reservoir of cGMP but remain saturated; the buffering by channels seems not to be appreciable (Gillespie and Beavo, 1989; Cobbs and Pugh, 1987).

For a stepwise change of GCy and PDE activity imposed on a steady-state with $v = 0$, the differential equation (5) may be solved by direct integration. The values of GCy and PDE are assumed to change abruptly to new stationary values at the boundary, with subsequent relaxation of s toward a new steady state. The boundary conditions for an initial steady state t_0, s_0; and a final steady state t_∞, s_i, yield a relation similar to Eq. 4:

$$\ln A = \ln\left(\frac{s_i - s}{s_i - s_0}\right) = -\frac{t - t_0}{T_i} \tag{6}$$

The dimensionless ratio A expresses the proportion of total substrate excursion remaining to steady state; this will be called the progress parameter, as it maps the entire course of the transition onto the interval (1, 0). The time constant T_i is the effective value of K_m/V over the integration interval, as altered for example by light activation or a PDE inhibitor.

The expression for the progress of substrate activity can be put in a form more conveniently related to membrane current and enzyme inhibitors. The substitutions $s_i = as_0$; $T_i = bT_0$; $j^p = s/s_0$ allow the substrate activity to be represented as a proportion of the initial value:

$$\ln A = \ln\left(\frac{a - j^p}{a - 1}\right) - -\frac{t - t_0}{bT_0} \tag{7}$$

The relation of the boundary value constraints a and b to enzyme inhibition is developed next.

Relations of Competitive Inhibitors

By definition, a competitive inhibitor I modifies the Michaelis relation in a distinctive fashion (Fersht, 1984, p. 108):

$$v = \frac{V}{1 + \left(1 + \frac{I}{K_i}\right)\frac{K_m}{s}} \approx \frac{sV}{\left(1 + \frac{I}{K_i}\right)K_m} \tag{8}$$

where K_i is a characteristic constant. As before, the linear approximation is s applies for $s \ll K_m\,(1 + I/K_i)$, so that the time constant T is replaced in inhibitor by the value $T_i = (1 + I/K_i)T$. Given this restriction, the remarks that follow also apply equally well in the case of noncompetitive inhibition. The linear approximation can be put in a reciprocal form,

$$\frac{1}{v} \approx \left(1 + \frac{I}{K_i}\right)\frac{T}{s} \tag{9}$$

which yields straight line plots of $1/v$ vs. I under conditions of constant substrate and enzyme activity. This plot is useful to evaluate competitive inhibitors (Dixon, 1953).

The problem of a rod initially at steady-state suddenly thrust into inhibitor can now

be stated. Reserve K_i to refer to PDE inhibition by a given agent; assume for argument some similar inhibition with constant K'_i applies to GCy, so that its velocity becomes GCy/(1 + I/K'_i). Solutions for the steady-state boundary condition in the presence of inhibitor, assuming constant PDE and GCy activation, are found by evaluating Eq. 5 with $v = 0$:

$$s_i = \frac{1 + \frac{I}{K_i}}{1 + \frac{I}{K_i}} s_0; \quad T_i = bT_0 = \left(1 + \frac{I}{K_i}\right) T_0 \tag{10}$$

Note that only PDE inhibition affects the time constant T_i whether or not GCy is affected as well. The possible effects on PDE and GCy are classified by the relation of the boundary constraints a and b:

$a = b = 1 + \frac{I}{K_i}$: inhibition, PDE only

$a < b > 1$: inhibition, both PDE and CGy

$a < b = 1$: inhibition, GCy only

$a < b$: inhibition of PDE and stimulation of GCy

Unsuspected partial inhibition of GCy when only inhibition of PDE is considered leads to an underestimate of PDE activation.

Lifetime of Activated PDE

In darkness most of the PDE in a rod is inactive. A simple hypothesis for the light-activated species PDE* is exponential decay to an inactive form with the time constant T_{PDE^*}.

$$\frac{\text{dPDE}^*}{dt} = -\frac{\text{PDE}^*}{T_{PDE^*}} \tag{11}$$

If PDE* is produced in linear proportion to excited rhodopsins R*, then Eq. 11 may be restated using units of isomerizations. Let L = dPDE*/dt be the continuous light intensity in isomerizations s^{-1} sufficient to establish a steady-state with activation designated PDE*; let F be the strength in isomerizations of an impulsive flash just sufficient to produce the same activation PDE*. Rearrangement of Eq. 11 gives T_{PDE^*} in terms of measurable quantities:

$$T_{PDE^*} = \frac{F}{L} \tag{12}$$

RESULTS

The investigation developed in two parts. The first described the reactions of current to perturbations by light or inhibitor, the second the relation of light intensity and inhibitor concentration at constant current. The initial experiments tested the approach via an enzyme inhibitor on the dark-active PDE, using IBMX-induced

current transients; the same method then applied to light-activated PDE. Subsequently, we explored the relation of light intensity and inhibitor concentration at constant membrane current, interrupting a possible current-related feedback loop. This approach defined the dynamics of PDE activation and deactivation in relation to current magnitude and adaptation by background light.

Dark-Active Phosphodiesterase

The reaction of rod membrane current to a jump of inhibitor concentration in the dark developed in three distinct phases (Fig. 3). In the first portion, the slope of current vs. time was steep. The onset of current growth followed the transition to IBMX without definite lag, the rate of rise being maximal within 50 ms as judged from a simultaneous junction current. In the middle segment, the slope lessened producing a definite kink in the growth curve. In the final portion, current resumed the basal value after the return of the cell to control Ringer's solution. The return transition was delayed by a mechanical lag which included the distance by which the Ringer's-IBMX boundary had advanced past the cell; the current followed a biphasic waveform with a rebound. The IBMX-induced current was light-sensitive throughout all segments.

The rate of current growth varied as a function of IBMX concentration in the following way: the slope of the initial segment saturated with increasing concentration, whereas within the plateau, both the slope and the maximal current changed progressively with concentration (Fig. 3 *A*). We postulated that the first changes in membrane current induced by IBMX might result only from changes in PDE inhibition (affecting the size of the free cGMP pool), uncomplicated by the additional consideration of feedback inhibition.

The concentration dependence of the initial rate of current growth in IBMX supported the notion of a saturable form of enzyme inhibition. A Dixon plot of reciprocal velocity at constant substrate (Eq. 9 and Fig. 3 *B*) was compared to the predictions of an isolated inhibition of dark-active PDE with GCy velocity constant, K_i 38 μM:

$$\frac{v_0}{v} = 1 + \frac{I}{K_i} \tag{13}$$

Some departure from this relation was noted over the full range of inhibitor concentration, hardly surprising in view of the crude estimate of initial velocity by a mean value (see caption). The partial success of this approach motivated the more exact treatment of a transition between steady-states; see Theory section, Eqs. 5–10.

The time dependence of the IBMX-induced current conformed to an exponential relaxation of cGMP activity. Plotted on a logarithmic scale (Fig. 3 *C*), data at all concentrations could be fit to straight lines by a single adjustable parameter (K_i), which specified the nature of enzyme inhibition. The course of current after a jump into inhibitor at $t_0 = 0$ was predicted from Eq. 7:

$$\ln A = \ln \frac{a - j^p}{a - 1} = -\frac{t}{bT_0} \tag{14}$$

where T_0 is the time constant of PDE hydrolysis without inhibitor; A varies from 1 to

0 (see Theory section, Eq. 6 and following text). For $a = 1 + I/K_i$, $K_i = 32$ μM, current followed this relation with remarkable fidelity over the first 200 ms after the inhibitor jump.

The apparent relaxation time ($1/e$) of cGMP after an inhibitor jump varied with concentration; PDE inhibition predicted a particular dependence on concentration:

$$T = bT_0 = \left(1 + \frac{I}{K_i}\right) T_0 \tag{15}$$

(Eq. 8 and after). The times given by the reciprocal slopes of the logarithmic plots (panel *C*) followed this relation closely, panel *D*. This plot determined two quantities: K_i, from the reciprocal slope, and T_0, from the intercept at $I = 0$. The value found for K_i (32 μM), matched the result of Fig. 3 *C*.

The velocity of PDE in darkness without inhibitor determines the basal time constant for cGMP hydrolysis, T_0. From the mean across cells, the free cGMP pool undergoes 2.8 *e*-fold exchanges per second in darkness (Table II). Even in darkness cGMP hydrolysis is so rapid that in many individual cells cGMP activity follows changes in PDE activity with lag ~200 ms. These observations agree with other metabolic measurements of cGMP in situ, but oppose the simple view of dark rod PDE as an inactive enzyme awaiting light activation, see Discussion, subsection *Dark-Active PDE.*

A process possibly related to feedback regulation of the cGMP pool could be separated from the time constant of PDE hydrolysis on a logarithmic plot (Fig. 3 *E*). The plots in different concentrations of IBMX were scaled to a single curve by the factor $b = (1 + I/K_i)$, predicted from Eqs. 14 and 15. All curves bent from the initial log-linear relation at about the same time, despite the large differences in current magnitude. This behavior is consistent with a feedback stage involving an apparent time constant of 200 ms, independent of PDE. If the delay owes to down-regulation of GCy, the observation provides a constraint on the time course. Finally, the constancy of the second segment of the progress curve at low [IBMX] follows the proposal of Hodgkin and Nunn (1988), which predicts only small decrements in cyclase velocity for small increments of resting dark current.

The return course of current after a jump back out of IBMX and into Ringers presented other evidence suggesting a feedback process (Fig. 3 *A*). The lag until the current again reached the basal level (first crossing) grew progressively with inhibitor concentration; the extent of the undershoot grew also, but toward a limit. Thus an influence related to inhibitor concentration persisted after the rod left the IBMX solution. These curves invited comparison to the similar family produced by a series of flashes of graduated intensity presented to rods loaded with a calcium chelator (Torre et al., 1986). This problem arose also in relation to step light stimuli and adaptation; for the moment, we note merely that IBMX provoked a transient oscillatory reaction of light-sensitive current without light or exogenous Ca buffer.

A possible effect of IBMX on GCy was delimited. The effect of inhibition of GCy in addition to PDE was calculated, assuming a competitive mechanism (Eq. 10). The boundary constraint a took a more complicated form, $a = (1 + I/K_i)\,(1 + I/K_i')^{-1}$. If K_i' is the inhibitory constant for GCy, then values of $K_i' < 30\ K_i$ could reasonably be excluded on inspection; this boundary case is presented for comparison (Fig. 3 *F*). As

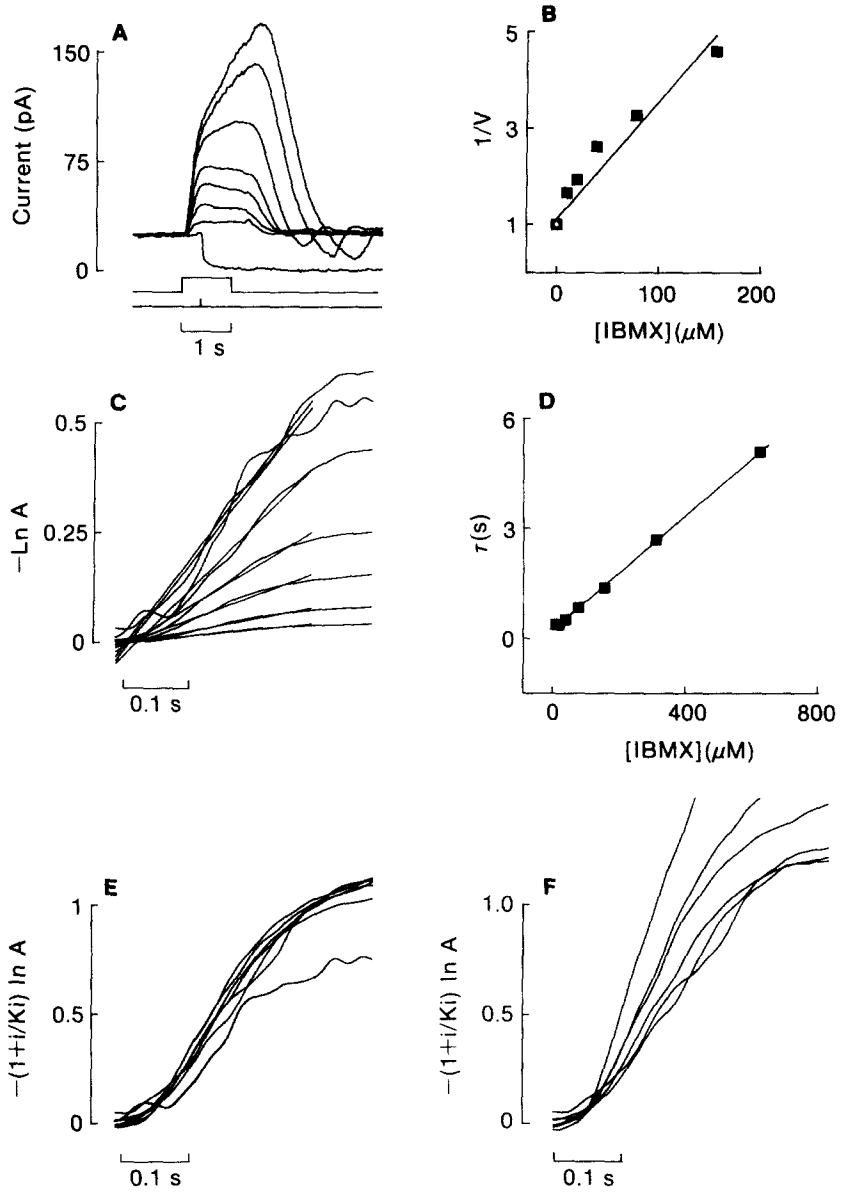

FIGURE 3. Dark current progress vs. IBMX concentration. (*A*) Collected records of rod dark current on jumps from Ringer's into inhibitor of concentration *I*, increased in twofold steps from 10 to 625 μM. Pipette-inward current is plotted up, zero defined in saturating light. The bottom record is the control response to a saturating flash of 2×10^4 isom after a jump into plain Ringer's. The timing trace (below) marks onset of the jump (step) and flash (tick). The initial slope of dark current growth in IBMX approached a limit with increasing concentration. Cell 1. (*B*) Reciprocal velocity vs. IBMX concentration. The data of *A* were plotted as reciprocal

reaction velocities v_0/v, using the transformation

$$\frac{v_0}{v} \approx \frac{s_{max} - s_0}{s_{max} - s} = \frac{J^p_{max} - J^p_0}{J_{max} - J^p}$$

where J_0, J, J_{max} are currents measured 200 ms after the jump in 0, intermediate, and 1 mM inhibitor; the exponent $p = 1/h = 0.5$ is the reciprocal Hill coefficient for activation of current by cGMP. The fraction approximates $v = ds/dt$ by a chord slope; the scale is normalized by the control velocity in the absence of inhibitor, v_0. Solid line, least squares regression forced through (0, 1), open point; apparent K_i 38 μM. Some deviation is apparent from the linear relation predicted for competitive inhibition of PDE. (*C*) Logarithmic transformation of data in *A*. A model postulating stepwise inhibition of PDE predicts an exponential transition of cGMP activity s between initial (s_0) and inhibited (s_i) steady-state values (Theory, Eq. 6). Logarithmic plots of the quantity $A = (s_i - s)/(s_i - s_0)$, which varies from 1 to 0 as s goes from s_0 to s_i, should give straight lines. Competitive PDE inhibition predicts the concentration dependence in IBMX: $s_i = a\, s_0 = (1 + I/K_i)s_0$, Theory, Eq. 10. Current relates to cGMP activity by the equation $s/s_0 = (J/J_0)^p = j^p$. Records of A are plotted according to the transformation,

$$\ln A = \ln\left\{\frac{s_i - s}{s_i - s_0}\right\} = \ln\left\{\frac{a - s/s_0}{a - 1}\right\} = \ln\left\{\frac{a - j^p}{a - 1}\right\}$$

The curves illustrate $K_i = 32$ μM, $p = 0.5$. Straight line segments are least squares regressions to each curve of transformed data over the 200-ms interval after inhibitor onset; the lines have been extrapolated beyond this interval by arbitrary amounts for comparison. A restricted set of values for K_i and p yielded straight-line behavior; for a given p, a best value of K_i was chosen based on least squares regression (which matched the fit by eye). For $p = 0.5$, $K_i = 32$ μM; $p = 0.33$, $K_i = 17$ μM. Values of $p > 0.7$ were rejected because all curves diverged. The agreement with an exponential transition is satisfactory for the initial 200 ms; subsequently, all responses departed from a linear relation, possibly indicating onset of feedback regulation of guanylyl cyclase. Note that the steep noisy trace corresponds to the smallest signal, ~5 pA in 10 μm IBMX. (*D*) Exponential time constants vs. IBMX concentration. The reciprocal slopes of the curves in *C* (approximated from the linear regressions) correspond to the exponential time constants T for the change of cGMP activity in inhibitor. Competitive inhibition by IBMX predicts the relation $T = (1 + I/K_i)T_0$; the solid line is the least squares regression with $T_0 = 0.23$ s at IBMX = 0, $K_i = 32$ μM. (*E*) Scaling relation of dark currents induced by IBMX. The records of A are plotted with the transformation $b \ln A = (1 + I/K_i) \ln A$ (Theory, Eqs. 7–10). For the first 200 ms after the IBMX jump, the records nearly superimpose; the noisy record (10 μm IBMX) lies somewhat below the others. Results are consistent with a singly-exponential relaxation along the line $(1 + I/K_i) \ln A = -(t - t_0)/T_0$. Observations over the concentration range 0.01–1 mM inhibitor are adequately described by a single $K_i = 32$ μm. (*F*) Scaling relation of dark current relaxations in IBMX, effect of assuming combined inhibition of both guanylyl cyclase and PDE by IBMX. The inhibitory constant K'_i for guanylyl cyclase was taken to be 30-fold greater than the inhibitory K_i for PDE. For competitive inhibition of both PDE and guanylyl cyclase, $s_i = a\, s_0 = [(1 + I/K_i)/(1 + I/K'_i)]\, s_0$ (Theory, Eq. 10). The records of *A*, IBMX 20–625 μM, were plotted according to the resulting expression for $(1 + I/K_i) \ln A$ (see text), with $p = 0.5$, and $K_i = 32$ μm, as in *C*. At inhibitor concentrations 20–78 μM, far below K'_i, the behavior was substantially the same as in *E*. As the concentration of IBMX increased, the observations diverged progressively from the predicted exponential relaxation with time constant $(1 + I/K_i)T_0$; hence the model with competitive inhibition of guanylyl cyclase was rejected for $K'_i < 30\, K_i$.

expected, the predicted relaxation time constants for $I \ll K_i'$ converge to the results expected in the absence of cyclase inhibition.

For inhibitor concentrations >1 mM, possible evidence of GCy inhibition emerged. As the outer segment returned to Ringer's after exposure to inhibitor, a sudden increase in the light-sensitive current often occurred (Fig. 4). This finding contradicted the fall in current expected from the reversal of PDE inhibition, always observed at lower IBMX concentrations. Actions of IBMX other than the intended

TABLE II

Rod Properties from IBMX Jumps

Cell	J_d	D	R_{cGMP}	T_{PDE^*}	Figure
	pA	*isom* s^{-1}	s^{-1}	*s*	
1	25		4.35		2 *A*, 3, 5
2	27		3.33		2 *B*
3	28		8.60		6, *A* and *B*
4	38		2.63		7
5	49	416	3.10		4, *A–D*
6	30	944	1.85	0.88	8, *A* and *B*, 9 *A* and *B*
7	39	256	0.91	0.88	10, *A–D*, 11, *A* and *B*
8	25	1,696	1.45	0.55	
9	20	834	1.68	0.88	
10	35	2,095	2.53	0.88	
11	35	3,304	8.26	0.88	
12	45	267	0.94	1.1	
13	35	670	2.44	0.88	
14	21	169	0.75	0.88	
15	25	530	1.59	0.88	
16	25	3,376	2.94	0.55	
17	25	268	3.92	0.88	
18	49	338	0.82	0.55	
19	40	334	0.41	1.1	
20	21	542	3.57	1.39	
Mean	32	1,002	2.8	0.88	
SD	9	1,023	2.2	0.21	
N	20	16	20	15	

J_d, dark current at jump onset; D, dark PDE activity measured in units of equivalent light-activated enzyme, as $(K_i/I)L$ (Fig. 8); R_{cGMP}, rate constant of dark cGMP hydrolysis, from $(1 + I/K_i)/T$, with T the exponential time for the substrate transition after a dark jump into IBMX, (Fig. 3, *C* and *D*); T_{PDE^*}, apparent lifetime of light-activated PDE, from (flash strength/light intensity), Fig. 9.

inhibition of cyclic nucleotide phosphodiesterase have been reported, including effects mediated by adenosine receptors and GCy (Beavo et al., 1970; Strinden and Stellwagen, 1984; Pepe et al., 1986; Williams and Jarvis, 1988). IBMX is stated not to affect the cGMP-dependent conductance of excised membrane patches (Nakatani and Yau, 1988*a*). Most of this investigation was restricted to the range $I < 30\ K_i < K_i' < 1$ mM, where the effect on GCy could be neglected.

In summary, the immediate effects of IBMX in darkness are consistent with PDE inhibition, K_i 30 μM, and with dark active PDE sufficient to turn over the the outer segment pool of exchangeable cGMP in 0.6 s or less.

Light-activated PDE

*Flash stimuli.*The facile control of dark-active PDE with inhibitor concentration jumps brought up the idea of resolving the kinetics of PDE light activation by a similar method. The response of current to brief saturating flash stimuli was investigated first, to define the onset of IBMX-induced inhibition of the light-activated PDE. Attention focused on the interval just after a jump into inhibitor, when internal conditions of the rod were not much changed from the resting dark state. In these experiments the inhibition of the initially dark-active enzyme still had to be considered.

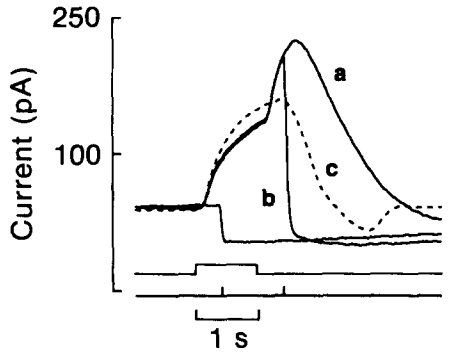

FIGURE 4. Dark current progress, 5 mM IBMX. The effect of 5 mM IBMX on dark current. Progress curves in 5 mM IBMX (solid, *a* and *b*) at first overlay the course in 156 μM inhibitor (dashed), but then lagged behind, suddenly increasing on the return to control Ringer's. The anomalous current increase was light sensitive (flash, *b*). A control record in Ringer's (unlabeled, no IBMX) defined the light-sensitive current magnitude. The bottom traces mark timing of jump (step) and flash (ticks). Flash strength $6 \times 10^{+5}$ isom. Cell 5.

The flash response in IBMX was delayed relative to control responses in Ringer's (Fig. 5 *A*). This delay lengthened progressively with increasing concentration. For saturating flashes, transients observed at different concentrations were reduced to nearly the same form when scaled by the magnitude of the dark current. The normalized responses were superimposed by subtracting the delay (Fig. 5 *B*). Elevation of cytoplasmic cGMP by intracellular infusion does not produce such a delay (Cobbs and Pugh, 1985).

The simplest hypothesis for the delay of the flash response was that initially IBMX affected the saturating flash photocurrent by competitively inhibiting PDE without altering its light activation. This situation might arise, for example, if IBMX competed with cGMP at the hydrolytic site but not with the binding attachment of the inhibitory PDE_γ subunit. Thus the proportion of catalytic sites available for occupancy by substrate would change, but not the amount of enzyme activated by light. This scheme established a correspondence between PDE velocities occurring at the same time after a flash in the presence or absence of IBMX. If the wavefront of

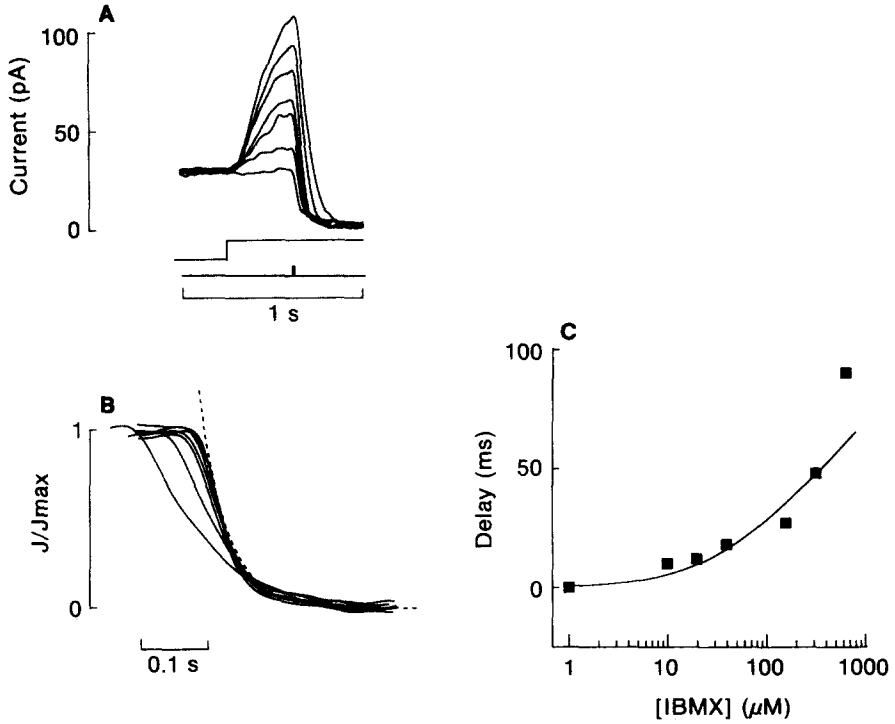

FIGURE 5. Saturating flash responses vs. IBMX concentration. (*A*) Collected rod membrane current light responses following IBMX jumps, obtained interleaved with the dark records of Fig. 3, [IBMX] 10–625 μM. The IBMX-induced current was light-sensitive. Membrane current transients were delayed progressively with increasing IBMX concentration. The timing trace (below) marks onset of the jump (step) and flash (tick). Flash strength $2 \times 10^{+5}$ isom, duration 20 μs. Cell 1. (*B*) Superposition of normalized flash responses. Light responses of *A* have been scaled by the dark current magnitude at stimulus onset and translated along the time axis by delay intervals d to overly the 30-ms exponential cell time constant (dashed line). With increasing inhibitor concentration the responses joined the exponential curve at later points; in 625 μM IBMX the response fell short of this envelope (deviant trace). (*C*) Light response delay vs. IBMX concentration. Delay intervals d of *B* plotted against [IBMX], logarithmic scale. Solid line, $T \ln(1 + I/K_i)$, with K_i 32 μM and T 20 ms, predicted by initial exponential growth of phosphodiesterase activity after a flash, subject to competitive substrate inhibition by IBMX.

light-activated PDE velocity is $W(t)$ in the control, and $W_i(t)$ in inhibitor and the delay of the normalized response in inhibitor is d, then:

$$W_i(t) = \left(1 + \frac{I}{K_i}\right)^{-1} W(t) + W(t - d) \tag{16}$$

To the extent that IBMX simply introduced a first-order delay d of the saturated flash response, this same scheme also established a correspondence between PDE velocities at different intervals after the flash. Eq. 16 described a function that transformed

a sum of arguments into a product, hence the function $W(t)$ was exponential:

$$W(t) = C \exp\left(\frac{t}{T_g}\right) \tag{17}$$

Here t was the time from onset, T_g the exponential time of PDE activity growth, C a nonzero constant. Now we can also solve Eq. 16 for the delay d as a function of inhibitor concentration I:

$$d = T_g \ln\left(1 + \frac{I}{K_i}\right) \tag{18}$$

The observed delay followed the predicted logarithmic relation (Eq. 18) over the entire range of IBMX concentration. The time constant T_g of PDE activation was independent of IBMX concentration, thereby strongly supporting the notion of inhibition of light-activated PDE velocity without effect on the course of PDE activation (Fig. 5 *C*). The apparent K_i of IBMX derived by this method for light-activated PDE could not be distinguished from the value obtained above for dark-active PDE, but accuracy was degraded by the small magnitude of the delay in the range $I < K_i$.

The delay of the flash response provided a scale with which to measure the onset of IBMX inhibition. Delay onset was more than half-complete within 50 ms, and complete within 100 ms, despite the continued growth of current (Fig. 6). Just as with intracellular cGMP infusion, the growth of current itself was not associated with flash response delay. From these observations, the onset of IBMX inhibition was simultaneous with the change of solution composition. Thus the observations with flash stimuli PDE supported the simple view that light and dark active PDE were inhibited in the same way by IBMX, which directly affected the rate of hydrolysis rather than events leading to PDE activation.

*Step stimuli.*The analysis of flash responses just given skirted several important issues, including feedback regulation and the possible effects of extended IBMX exposure apart from inhibition of cGMP hydrolysis. The use of step stimuli allowed these questions to be explored conveniently under steady-state conditions and suggested an approach to light adaptation.

When a jump was made into inhibitor simultaneous with a step of background light, the behavior of current depended on both concentration and intensity (Fig. 7). For each inhibitor concentration, a single value of light intensity could be found just sufficient to suppress the IBMX-induced current at steady-state (panel *B*). Such steady states were easily maintained for several minutes (not shown).

The correspondence between equal currents in differing conditions of light or IBMX extended beyond steady states at the resting value of current. The entire adaptive recovery of current in a steady background light was reproduced in IBMX by an appropriate selection of light intensity (panel *C*). The recovered current was light-sensitive. Such equivalent states of light-sensitive current always required brighter background light in the presence of IBMX. These observations supported the conclusion that the course of light adaptation, defined as the recovery of current in sustained light, depended only on outer segment current magnitude and PDE

velocity, but was independent of isomerizations. This statement applied over the range of light intensities which could be conveniently offset by IBMX, from darkness to ~4,000 isom s^{-1}. The observations all supported the simple view that after some initial transient the effect of IBMX on rod PDE remained constant.

The observations on light adaptation with step stimuli were consistent with reports using flash stimuli, if the different conditions of current were taken into account. Thus Cervetto and McNaughton (1986, toad) found that IBMX prolonged responses with increased dim flash sensitivity, but that this effect was antagonized by a steady background light sufficient to return current to the basal value. We found that as background steps were dimmed successively, current increased above the resting

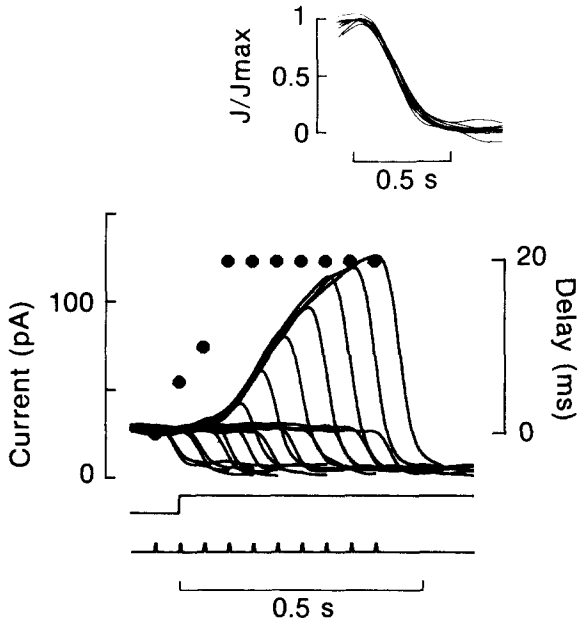

FIGURE 6. Onset of photocurrent delay in IBMX. (*A*) Collected rod membrane current responses to saturating 20-μs flash stimuli of 2×10^5 isomerizations, triggered at successive 50-ms intervals in relation to an IBMX jump (solid traces). At each stimulus interval, a control record (no jump) and an IBMX response were paired. IBMX introduced a response delay *d* relative to the control. Bottom traces mark onset of jump (step) and flashes (ticks). The delay times in IBMX (circles, right axis, see also *inset* in *B*) are plotted against time of stimulus onset. The delay time reached maximum within 100 ms, while current growth continued over a much longer period. IBMX 200 μM, cell 3. (*B*) (*Inset above*). IBMX jump flash responses superposed. Each IBMX response from *A* was scaled to unity and plotted against time from stimulus onset less a delay interval *d*, adjusted for best fit by eye.

dark level (Fig. 7 *B*). The initial transient oscillation of current became larger and decayed more slowly; ultimately the current was grossly unstable. Hence both investigations supported the view that in the presence of increased current light sensitivity increased in a manner not directly explained by PDE inhibition. Quantitative description required another approach; see below, *Light Adaptation* Eq. 23 and Fig. 7 *D*.

Experiments at Constant Membrane Current

The results to this point established that IBMX controlled PDE-mediated hydrolysis with sufficient range and precision to explore most of the physiologic range of light

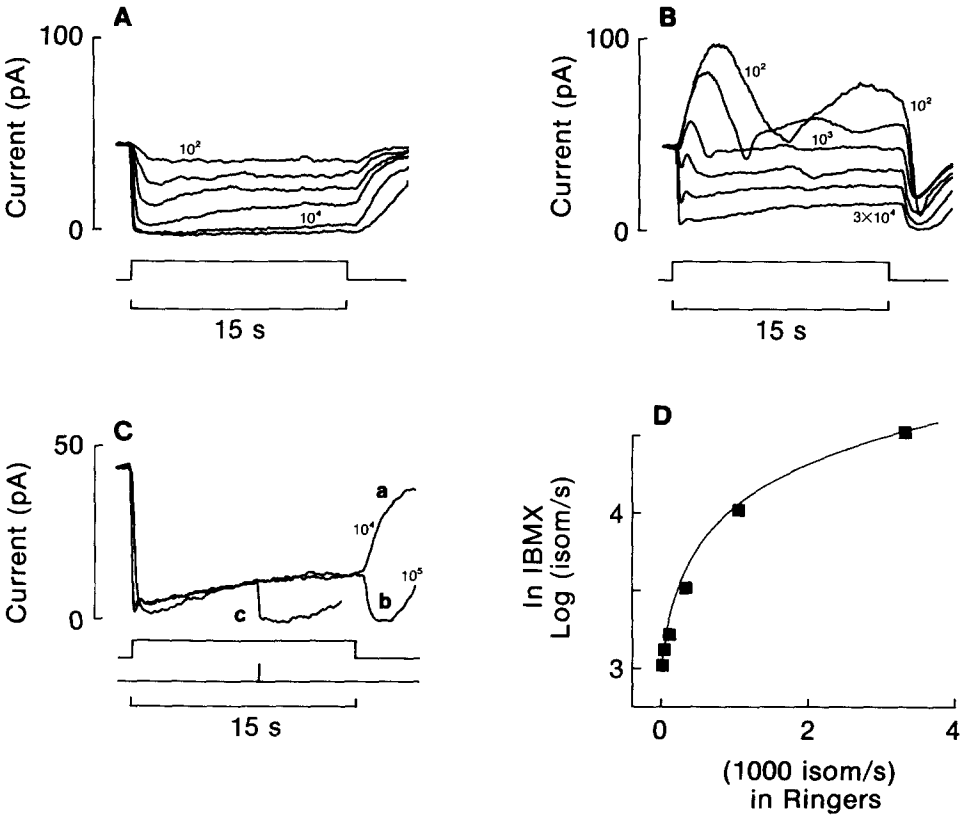

FIGURE 7. Adapting light steps and IBMX jumps. (*A*) Current responses to steady light steps, intensity graduated by factors of $10^{+0.5}$ from 1.0×10^2 isom s^{-1} (3.0 quanta μm^{-2} s^{-1}). The trials were interleaved with those of *B*. The notable recovery of current in constant light for stimuli of 3.3×10^3 and 1.0×10^4 isom s^{-1} exemplifies light adaptation. Dim flash sensitivity (responses not shown) 0.13 pA/isomerization. (*B*) Current responses to IBMX jumps simultaneous with light steps. In IBMX, more light was required to produce steady currents matching the control records in *A*. The light intensity which almost exactly counterbalanced the effect of IBMX in darkness at steady state was 1.0×10^3 isom s^{-1}. Current instability increased progressively through the region of dim steps and increased dark current. The timing trace at bottom marks both step and jump. IBMX 250 μM, cell 5. (*C*) Matched current traces demonstrating light-adaptive recovery of current at two different light stimulus intensities, one with and one without IBMX: (*a*) without IBMX, 1.0×10^4 isom s^{-1}; (*b*) with IBMX, 1.0×10^5 isom s^{-1}; and (*c*) with IBMX and a just-saturating test flash of 5.8×10^5 isom. Traces *a* and *b* followed the same adaptive course despite a 10-fold difference in isomerization rate. IBMX 250 μM, cell 5. (*D*) Light intensities from *C* required to match rod current responses in the presence or absence of IBMX, vs. [IBMX]. A step of steady light L' in IBMX was chosen to match the current produced by a light step L in control ringer. Squares, experimentally determined intensities L'; solid line, relation $L' = D(I/K_i) + L(1 + I/K_i)$, where D is dark PDE activity expressed in equivalent isomerizations s^{-1} and $K_i = 28$ μM.

stimulation; the second phase of the investigation defined the relation between stimulus light and PDE activation under conditions of constant membrane current. This constraint applied equally to both the source and sink of cGMP, although a description of PDE activation at constant cGMP and Ca activities was the main goal. In practice, the intensity of a light stimulus was adjusted to annul the change in current produced by a jump of inhibitor concentration. This procedure (a null method) established an equivalence with respect to the cGMP pool between conditions differing in light intensity and inhibitor concentration before and after the jump, assuming only that current was spatially uniform and a monotonic function in each variable.

Light Dependence of PDE Activity

The course of light-sensitive current followed a characteristic path after the simultaneous onset of an IBMX jump and a counterbalancing background light step, adjusted to yield no change of current at steady-state (Fig. 8 *A*). The current always increased at first, establishing that the effect of IBMX was more rapid in onset than that of light. The current transients were nearly congruent at different inhibitor concentrations, which suggested that the same principle of membrane current control applied for the relaxation of induced increases of dark current as for light adaptation (see *Light Adaptation,* and Fig. 7 *C*).

The major interest of these experiments was the dependence of light intensity on IBMX concentration (Fig. 8 *B*). If D is the dark and L the light-excited PDE activity, given in units of isomerizations rod^{-1} s^{-1}, then we may write an equation which expresses the fact that current is at steady state and the same both before and during inhibitor. If only PDE and not GCy is activated by light, then equality of both PDE velocity and substrate before and during IBMX inhibition required:

$$D = \frac{L + D}{1 + \frac{I}{K_i}} \tag{19}$$

which simplified to:

$$L = \frac{I\,D}{K_i} \tag{20}$$

The outstanding feature of this model of rod phosphodiesterase activity is linearity. Excitation by different isomerizations is independent; both light and dark activity sum independently. The observations closely followed this prediction, although at the highest IBMX concentration (1 mM) light intensity fell short of the linear prediction by 20%. The quantity D varied widely from cell to cell; for K_i 32 μM, the mean over 16 cells matched the activity excited by 1,000 ± 260 isom s^{-1}. The large value of dark active PDE supported the previous analysis of the relaxation time of IBMX jumps in darkness (Fig. 3).

What of the probability that IBMX effects on GCy or some other entity contribute to the observed relation of light intensity to inhibitor concentration? First of all, it is worth noting that the nonlinearity of the relation of channel gating to cGMP activity

is not involved; all the measurements were obtained at constant current. Second, the possible inhibition of GCy has already been examined above in relation to the evaluation of dark active PDE; the same arguments restricting the presumed inhibition constant K_i' apply here. Third, if GCy inhibition does occur, PDE activation

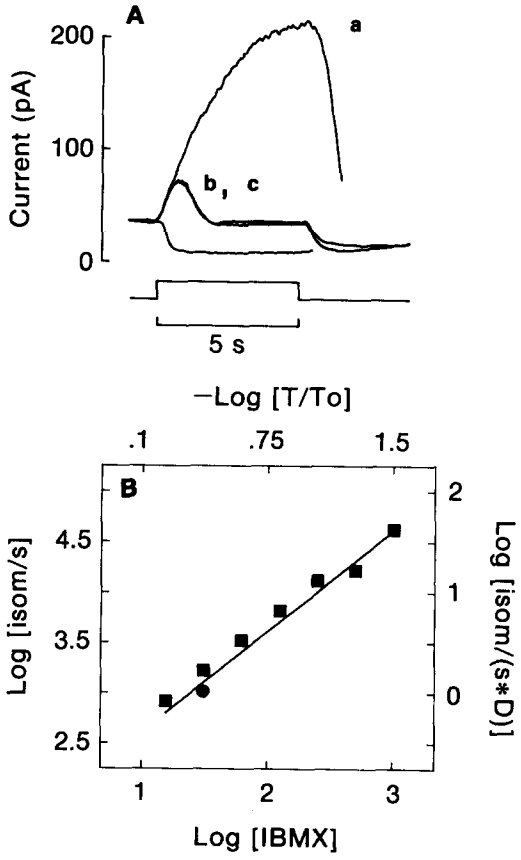

FIGURE 8. Light vs. IBMX concentration at constant current. (*A*) Current responses to IBMX jumps simultaneous with counterbalancing light steps. At each concentration, an intensity of steady light was chosen to just overcome the IBMX-induced current at steady-state (null method). Under this constraint, the initial transient currents were also nearly congruent, for [IBMX] >60 μM. Balanced states of light and IBMX were stable for more than a minute (not shown). Trace *a* dark, IBMX jump only; *b*, 2600 isom s^{-1}, and IBMX 125 μM; *c*, 4200 isom s^{-1} and IBMX 1 mM; unlabeled trace, light step only, 4200 isom s^{-1}. The timing trace at bottom marks both step and jump. Cell 6. (*B*) Steady light intensity required to just offset IBMX-induced current (see *A*), plotted against [IBMX] on logarithmic scales. Solid line, logarithm of the linear regression of the experimental points, slope 0.91 ± 0.04 (correlation coefficient in linear coordinates 0.98). The intercept corresponds to log (D/K_i) = log (54.6 isom s^{-1} μM^{-1}), predicted for competitive inhibition of PDE by IBMX with a single value of K_i for light and dark-active PDE species. The light intensity corresponding to the highest IBMX concentration (1 mM) fell short of the linear prediction by 20%. The top and right axes interpret the relation as an activation map of PDE. The right ordinate is calibrated in units of −log (isom s^{-1}/D), giving the proportional relation of the light stimulus range to the dark PDE activity. The top abscissa is calibrated in units of $-\log(T/T_0)$, where T is the time constant of substrate hydrolysis at a given light intensity and T_0 is the dark value, estimated by the method of Fig. 3. The filled circle marks the value of dark PDE activity, expressed as isomerization equivalents of light-activated PDE, and the corresponding time constant for substrate hydrolysis. The scales of right and top axes refer to values predicted in the absence of IBMX, under the condition of constant current.

will be underestimated at higher inhibitor concentrations. The estimate at the highest IBMX concentration (1 mM) does fall short of the linear prediction.

The possibility of light stimulation of GCy at constant current needs consideration. Recent results from Nichol and Bownds (1989), Rispoli and Detwiler (1989), and

Kawamura and Murakami (1989), suggest a light-dependent, Ca-independent form of adaptation, which might involve GCy or other components of the cascade. A more general form of Eq. 19 takes into account both possible light stimulation and IBMX inhibition of GCy, proceeding as before on the basis of equal cGMP activities at steady state before and during IBMX + light, and denoting light-activated GCy by $GCy_{h\nu}$:

$$\frac{GCy}{D} = \frac{(GCy + GCy_{h\nu})\left(1 + \frac{I}{K_i}\right)}{(D + L)\left(1 + \frac{I}{K'_i}\right)} \tag{21}$$

If we take $GCy_{h\nu} = (I/K'_i)GCy$, then Eq. 21 again follows. This relation strongly constrains light activation of GCy, but still admits appreciable stimulation in near-saturating light. The situation differs from the case of dark IBMX jumps, where the behavior of PDE could be discriminated confidently from the behavior of GCy, based on the dependence of the relaxation time constant for cGMP on inhibitor concentration. Inasmuch as the inhibition and light stimulation are supposed to cancel exactly, the apparent dependence of PDE activation on light is not altered.

The proportional relation of inhibitor concentration to the light required for constant current implies that PDE activation rises in linear proportion to light intensity. This relation contrasts sharply with the approximately hyperbolic dependence of current on background light met in the absence of IBMX. Consequences for the interaction of domains excited by individual isomerizations and the stoichiometry of the cascade will be deferred to the Discussion, subsection *Signal Dynamic Range and Adaptation.*

The relation of light to IBMX defined a map of activation for PDE in different conditions. (Fig. 8 *B*, right and top axes). The dark PDE activity (expressed as isomerizations s^{-1}) and its hydrolytic time constant made a natural scale on which to examine the variation of PDE activation with light intensity. The outstanding feature was the relatively modest range of activation, < 100-fold, reflected in whole rod PDE over the physiologic range of light stimulation. This finding, which roughly agreed with measures of cGMP metabolic flux, raised the issue of the relation between the signal and metabolic capacities of PDE, which required investigation of PDE activation under dynamic as well as steady-state conditions (see Discussion, subsection *Dark-Active PDE and Light-Active PDE*).

Lifetime of Light-activated PDE

The impulse and step responses of PDE light-activation were investigated at constant current. Steady-state PDE activation could be expressed as an equivalent rate of isomerization; likewise the number of simultaneous isomerizations (flash strength) necessary to fill the pool of activated PDE* to some initial value could be measured. If the strength of a flash F was adjusted to be just sufficient to fill the pool of PDE* to the steady level maintained by a background light B of simultaneous onset, then their ratio F/B was T_{PDE^*}; see Theory Eq. 12.

In practice, the velocity of PDE was abruptly diminished by a steplike onset of

IBMX inhibition. The extent of this velocity decrement depended on the IBMX concentration, *I*. This step of inhibition was counter-balanced by an increase of PDE activation produced by light. The membrane current transient after an IBMX jump and simultaneous light step was almost exactly annulled by a 20-μs Xe flash of proper intensity presented as the step began. The experiment is best understood by reference to the individual components (Fig. 9). At the null point, 1–2 pA of residual transient current remained, 3% of the response with the flash omitted.

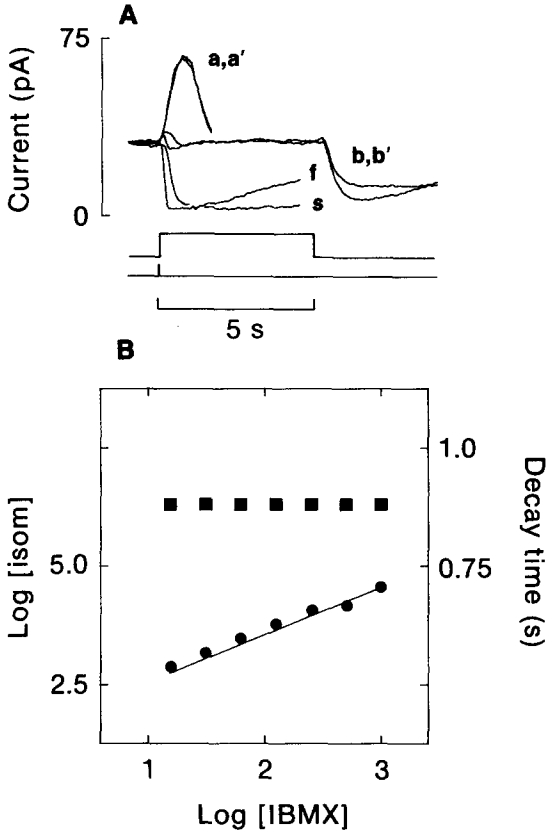

FIGURE 9. PDE lifetime at resting dark current. (*A*) Current responses to perturbations by IBMX and opposed light stimuli combining steady steps with 20 μs Xe flashes. Traces *a*, *a'* are from Fig. 8 *A* (2600 isom s^{-1}, IBMX 125 μM; 4200 isom s^{-1} and IBMX 1 mM); *b*, *b'* with flashes of 2,280 and 3,680 isom added at onset of light step (null condition); *f* flash only, 3,680 isom; *s*, step only, 4,200 isom s^{-1}; calculated PDE lifetime 0.88 s. The finite rise-time of the inhibitor concentration step produced a 10% underestimate of PDE* lifetime (not corrected); light stimuli were attenuated in units of 0.1 optical density. Cell 6. (*B*) Apparent PDE* lifetime vs. IBMX concentration. The null condition yielding the minimal change in current (see example *A*, *b*, *b'*) was explored over a series of inhibitor concentrations. The PDE* lifetime, T = flash strength/ step intensity, was plotted vs. [IBMX] (squares, right ordinate scale). The intensity of the counterbalancing light step (circles, left ordinate scale) is linear in [IBMX]. Solid line, linear regression with predicted slope D/K_i, where D is the dark PDE activity. Cell 7.

The apparent lifetime of light-activated PDE*, with current held at the resting dark value, was about a second. The mean value of T_{PDE^*} calculated from F/B was 0.88 ± 0.06 s (n = 15, 18°C). This result agrees with extrapolations from light scattering measurements by Dratz et al. (1987) and with a calorimetric estimate of transducin-stimulated GTPase in bovine rod outer segment suspensions (Vuong and Chabre, 1990).

Linear Range of PDE Activation

The hypothesis that the signal pathway from rhodopsin through activated phosphodiesterase decay is linear in isomerizations and strongly dominated by a single longest time constant was pursued over a range of IBMX concentrations (Fig. 9 *B*). The flash strength required to annul the transient current obeyed the same linear relation in IBMX concentration demonstrated previously for steady light steps (Fig. 8 *B*). The PDE lifetime T_{PDE^*} remained constant at 0.8 s over the entire range of IBMX concentration and light intensity. Thus at constant membrane current both the impulse and the step response of PDE activation and decay were nearly linear in isomerizations.

Light Adaptation

Next we investigated the relation of PDE regulation to light adaptation and membrane current. Interest focused on (*a*) the efficiency of light activation; (*b*) the apparent lifetime of the activated species; and (*c*) the behavior during the adapting transition. The experiments followed the approach just developed, with the addition of background light.

Over a range of background light intensities, *B*, jumps into IBMX at fixed concentration generated a family of progress curves (Fig. 10 *B*). The onset of IBMX-induced current generally resembled the curves generated by inhibitor jumps in darkness over a range of IBMX concentrations (Fig. 3 *A*), except that the resting current also varied with *B*. The resemblance would be expected if the important underlying parameter in both cases were PDE velocity, varied respectively either by graduated light activation or by IBMX inhibition. The behavior of current after offset of the inhibitor reinforced this notion. At lower background light intensities the recovery of current was biphasic, with a rebound. The behavior resembled the responses to IBMX in darkness (Fig. 3 *A*). At constant IBMX concentration, the lag time from IBMX offset to the rebound of current diminished with increasing light intensity.

Forti et al. (1989) simulated the light responses of rods loaded with calcium chelator (Torre et al., 1986). The marked current rebound was reproduced by a mathematical model, which postulated feedback limited to Ca-dependent GCy regulation. It is plausible to attribute our observations to the same feedback loop, but perturbed by an increase of current rather than a decrease. We did not analyze the phenomenon further, but point out that both situations involve a systematic variation of PDE velocity, in the one case caused by light, the other by inhibitor.

Curves describing the progress of rod GMP activity were derived from IBMX jumps in background light, just as before for jumps in darkness (Fig. 10, *C* and *D*). Because light increased PDE velocity, these experiments challenged the time resolution of the solution jump method. At higher light intensities the calculated hydrolytic rates fell far short of the prediction of linear dependence in light intensity and approached a limit. The limiting behavior was closely approximated by the effect of a single-pole low pass filter of time constant 50 ms, conforming to the rate measured for the change of solution composition using junction currents. This limitation was circumvented using the null method to study PDE activation at constant current, described below (Fig. 11 *A*), data plotted as circles in Fig. 10 *D*.

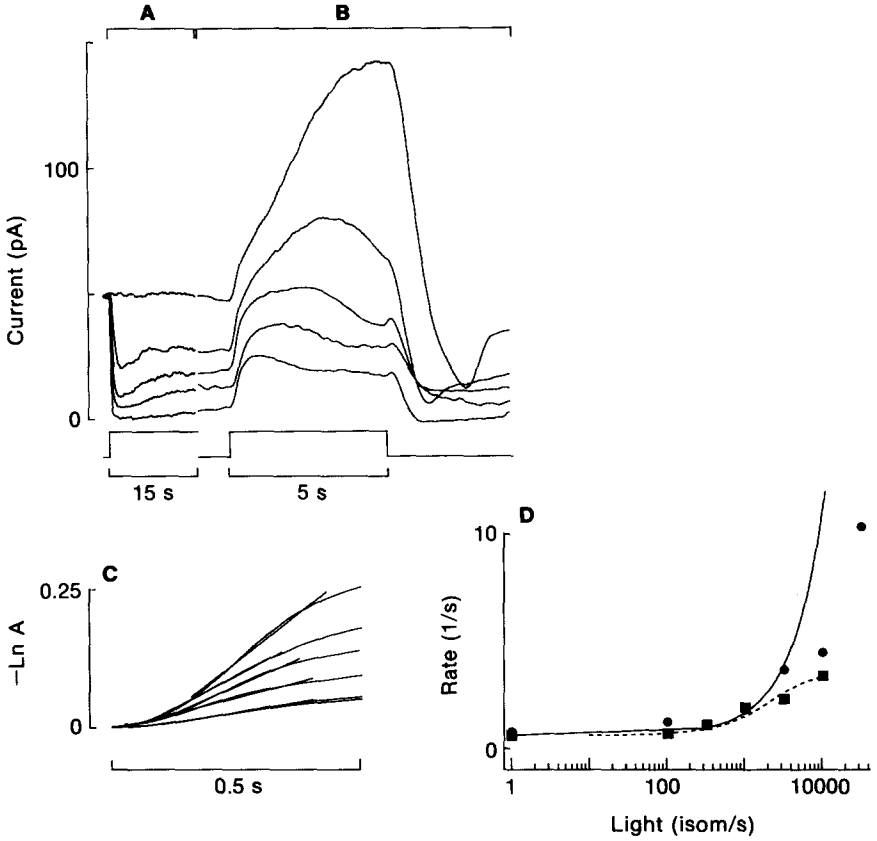

FIGURE 10. PDE activation in steady adapting light. (*A*) Current responses to steady light stimuli. Baseline trace dark; others, background light *B* graduated from 1.0×10^2 to 1×10^5 isom s^{-1} by factors of $10^{+0.5}$. Bottom trace, timing of light stimulus. Current reached steady-state within 15 s of light onset. Cell 8. (*B*) IBMX jumps in steady light. Responses to a jump into 125 μM IBMX after current had reached steady state in background light, companion records to *A*, same cell and light intensities. Bottom trace, timing of IBMX jump; note time base expanded compared to *A*. (*C*) Logarithmic transformation. The records of *B* were plotted according to the transformation

$$\ln A = \ln\left\{\frac{a - j^p}{a - 1}\right\}$$

as in Fig. 3 *C*. Competitive inhibition of PDE (both light and dark-active) predicts log-linear behavior vs. time. In bright light, the initial rate of rise was probably limited by the finite time for the change of solution composition. Straight line segments are least squares regressions to individual curves over the initial 200-ms interval following the jump; the lines were suppressed near the origin for clarity and have been extrapolated beyond the regression interval by arbitrary amounts for comparison. K_i 32 μM, p 0.5, IBMX 125 μM. (*D*) Hydrolytic rate vs. light intensity. Reciprocal slopes R of the curves of *C* (squares) are compared to the prediction for linear PDE activation by light, $R = 1/T = (1 + B/D)/(1 + I/K_i)T_0$, solid line. The dashed trace indicates the expected effect of a limiting low-pass filter of time constant 45 ms on the linear prediction. From steady-state measurements (see Fig. 11 *A*), PDE activation was predicted to follow the relation, K_iL/ID, plotted as circles.

We investigated the possible variation of PDE activation or decay with light adaptation, with observations at constant current. The experiments amounted to a series of constant current transitions into (IBMX + flash + light step) as before, but now in the presence of an additional steady background light of intensity B, which

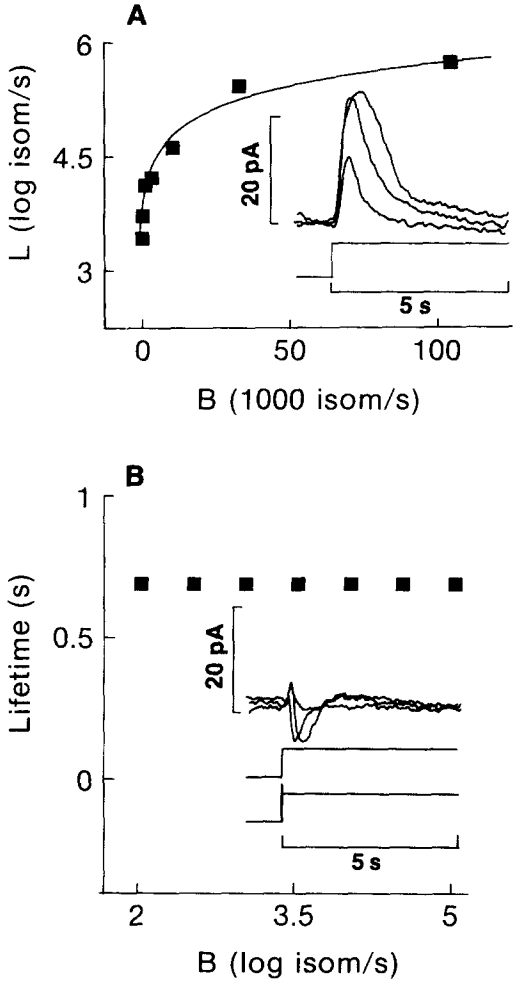

FIGURE 11. PDE lifetime in steady adapting light. (*A*) The intensity L of a superimposed light step just able to annual the IBMX-induced current at steady state is plotted against continuous steady background intensity B, extending the method of Fig. 8 *A*. Solid line, $L = (B + D)(I/K_i)$, expected for independent linear summation of newly-imposed step and steady background PDE activity, with D the equivalent dark PDE activity expressed as isom s^{-1}. Semilog presentation emphasizes the region of dim background stimuli. D 120 isom s^{-1}, K_i 31 ± 13 μM. (*Inset*) Collected current transitions for background light intensities of 3×10^2, 10^4, and 10^5 isom s^{-1}. Cell 8, continues experiment of Fig. 10. (*B*) In the presence of the background light B, jumps producing minimal transient current (null) were constructed according to the method of Fig. 9 *A*. A 20-μs Xe flash impulse of strength F was presented at onset of the IBMX jump and a simultaneous light step L. The PDE lifetime $T = F/L$ remained constant over the range of background light intensity B and light-sensitive current magnitude $0 < J < 50$ pA. The integrity of the adaptive recovery of light-sensitive current was verified before and after each set of trials. (*Inset*) Collected current transitions at the null condition for background light intensities of 3×10^2, 1×10^4, and 1×10^5 isom s^{-1}; timing trace marks simultaneous inhibitor concentration jump and light step with Xe flash at onset (tick). Cell 8.

varied from darkness to current saturation (Figs. 10 and 11). The background suppressed a given fraction of resting dark current, maintaining constant light adaptation. The inhibitor concentration, flash strength F, and light step intensity L were chosen such that the jump produced no change in current. In practice, to

achieve an exact null the timing of the IBMX jump relative to the flash and light step also had to be adjusted by an interposed delay of about 20 ms per twofold concentration increment. This delay is predicted from Eq. 18, which describes the delay of a flash photocurrent response in IBMX. When the adjustment of the delay was inexact, the position of the null with respect to flash strength could still be judged reproducibly within 0.1 optical density units, although a measurable transient current remained (Fig. 11 *B*, *inset*).

The simplest hypothesis made PDE light-activation and decay each independent of both membrane current and light adaptation. In this case the potentially different forms of activity—dark PDE activity, PDE activated by light from previous darkness, and PDE activated in the presence of an adapting light—all summed linearly with equal weight. The expression relating inhibitor concentration to light intensity then took a simple form for constant current jumps in background light. Since background light and dark activity sum independently, Eq. 19 can be rewritten:

$$L = \left(\frac{I}{K_i}\right)(B + D) \tag{22}$$

Equality of substrate and PDE velocity before and during IBMX is assumed.

The apparent PDE activity followed the predicted linear relationship in light closely over nearly the entire range of adapting background light intensity (Fig. 11 *A*). The K_i, 31 ± 13 μM, was determined as in Fig. 8. The PDE activity recruited per isomerization was nearly the same in the presence of a background light as in darkness. The signal range of the isolated rod from darkness to a saturating adapting background corresponded more or less to a 10-fold increment of PDE activity. This proportional range, however, depended on the apparent dark level of PDE activity, which was rather variable from cell to cell.

At the highest light intensities, the balancing light required in IBMX was somewhat less than the linear prediction. An accumulation of bleached photopigment which contributed to D via bleaching adaptation might be expected to produce just this effect. In any event, the magnitude of the residual light-sensitive current limited the accuracy of the measurement in this region.

The same series of experiments yielded the apparent PDE lifetime, given by the ratio (flash strength)/(step intensity). The apparent lifetime was constant at 0.9 s throughout the range of light adaptation, up to background intensities of 3×10^5 isomerizations s^{-1}. Steady background light and the concomitant changes in cytoplasmic cGMP and Ca^{2+} did not change the apparent rate of PDE decay.

Observations made at constant current supported the view that stages up to and including PDE decay were largely independent of light adaptation. Other things being equal, the simplest hypothesis predicted that PDE velocity and membrane current sufficed to determine the course of light adaptation as determined from membrane current.

This hypothesis may also be evaluated for conditions of changing membrane current and adaptation by returning to the observations of Fig. 7. This experiment compared current responses to two steps of different light intensity. A superimposed IBMX step was able to produce the same adapting course of membrane current in the two cases. These observations implied that PDE regulation, for both activation

and decay, remained constant during the progress of light adaptation as well as under steady conditions of constant membrane current. The data met a quantitative test through the predicted relation of light intensity and IBMX concentration.

For two light steps of intensity L and L' producing the same current trajectory, one with a concurrent IBMX jump, equivalence of both substrate activity and PDE velocity in the two cases required:

$$\frac{L' + D}{1 + \frac{I}{K_i}} = L + D \tag{23}$$

which simplified to:

$$L' = \left(\frac{I}{K_i}\right) D + \left(1 + \frac{I}{K_i}\right) L \tag{24}$$

Here L' was the light intensity required in the presence of IBMX, L the intensity without IBMX, and D the dark active PDE measured in units of equivalent isomerizations. Note that the relation is unchanged if a concurrent flash of strength TL or TL' is superimposed at light onset to produce stepwise changes in PDE activity. The close agreement of prediction and data supported the view that PDE activation remained a linear function of isomerizations throughout the course of light adaptation (Fig. 7 *D*).

DISCUSSION

Visual Cascade Overview of PDE

The concept of rod PDE as a signal enzyme evolved in relation to the function of light-activated PDE in the visual cascade. If the idea extends to the dark-active PDE, we can describe certain features of rod signaling in a unified way. Before we take up the detailed interaction of the metabolic and signal functions of the enzyme, the sequential relation of PDE to other elements of the cascade should be reappraised. Consider the conventional cascade scheme, especially the parts in boldface:[1]

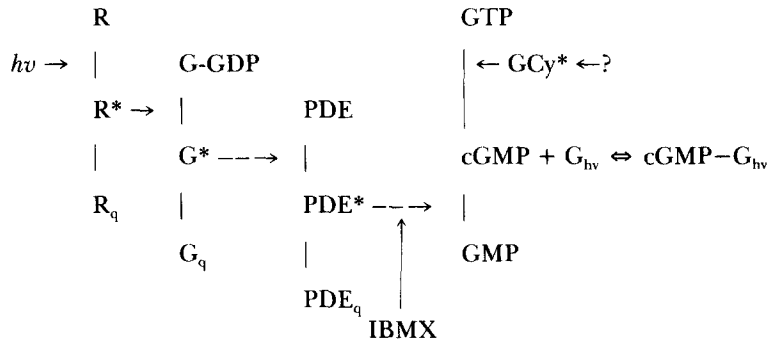

[1] The symbols * and q denote active and quenched (inactive) forms, | a transformation which may be reversible and occur by more than one route, → an increase reaction rate. This light-dependent scheme has been widely accepted (Pugh and Cobbs, 1986; Liebman et al., 1987; Stryer, 1988; Chabre and Deterre, 1989).

This concept is entirely light-dependent; without isomerized rhodopsin (R*) the activated forms of G protein (G*) and diesterase (PDE*) fall to zero concentration. The scheme fails to explain the regulation and signal function of the dark-active PDE, regulation of the dark current, or the dynamic signal range of the rod. These topics will be addressed under individual subheadings and correlated at the conclusion.

Several observations locate both PDE and the effects of IBMX in relation to kinetic features of the cascade. First, competitive substrate inhibition describes the dependence in IBMX concentration, so that action at the PDE catalytic site is likely (Figs. 3, 5, and 8). Secondly, along the signal path the serial position of the IBMX-sensitive site comes after the preponderant light-regulated site. This conclusion follows from the observation that the effects of IBMX on current precede those of light (Fig. 8 *A*). Thirdly, the dominant feedback regulatory site (of whatever identity) comes after

TABLE III

Comparison of Light and Dark Active PDE in Rods

Quantity	Unit	Dark	Light
K_i	μM	30	30
K_m	μM	130*	580‡
K_{cat}	s^{-1}		2,000§
E_0	μM	0.3‖	100¶
R_{cGMP}	s^{-1}	2.8	3.8×10^{-3}**
T_{PDE^*}	s	0.9	

K_i, IBMX inhibition constant; K_m, Michaelis constant; k_{cat}, turnover number; E_0, PDE copy number; R_{cGMP}, rate constant of cGMP hydrolysis in situ; T_{PDE^*}, apparent lifetime of activated PDE.

*Kawamura and Murakami, 1986*a*.

‡Barkdoll et al., 1988.

§Baehr et al., 1979.

‖Calculated from activity in situ.

¶Appelbury and Chabre, 1986.

**Table II, mean *R/D* 3.8 + −0.9 (n = 16); units s^{-1} $isom^{-1}$ s^{-1}.

Unreferenced entries, present work.

PDE on the signal path. The independence of both PDE activation and lifetime with respect to membrane current amplitude and the linear relation of PDE activation to isomerizations all support this last conclusion.

Enzyme–Substrate Relations

The substrate interactions of PDE link its metabolic and signal functions. Findings for rod PDE are summarized in Tables II and III. We will review kinetic parameters affecting cGMP hydrolysis in relation to prior work with emphasis on the significance for signaling.

The metabolic flux of the free cGMP pool and the activation of PDE should be strongly coupled, because they involve the same time constant, $T = s/v$. With dark cGMP activity 5 μM, T 0.6 s, our results predict a dark flux of 8 μM s^{-1}. Goldberg et al. (1983) measured retinal cGMP hydrolysis in situ based on the incorporation of ^{18}O

in the α-phosphoryl of GMP from $H_2{}^{18}O$; in toad the dark cGMP flux was ~2 μM s^{-1} (Dawis et al., 1988).[2] The increase of cGMP metabolic flux from darkness to saturating illumination is in rough accord with the proportional increase of PDE activity measured here, ~10-fold (Dawis et al., 1988). A more exact reckoning would have to take into account the variation of cGMP and GCy activity through states of light adaptation.

The K_i and K_m of PDE describe interactions of inhibitor and substrate at enzyme binding sites. The value for K_i reported here, 32 μM light and dark, differs modestly from reports by other methods in purified cattle PDE (10 μM, Baehr et al., 1979) and salamander in vivo (7 μM, Hodgkin and Nunn, 1988). Dark- and light-activated forms of PDE could not be distinguished on plots of IBMX concentration vs light intensity at constant current, which are straight lines (Figs. 8 *D* and 10). The point is of interest in view of reports that PDE isoforms may sometimes be distinguished by inhibitory constants differing by >10-fold (Reeves et al., 1987). Whether the Michaelis constants of light and dark active PDE are distinct or equal has been disputed (Kawamura and Murakami, 1986*a*); here we find only that both are probably much greater than prevailing substrate activity.

The K_m has a particular significance for the messengers of hydrolytic enzymes which signal by amplitude modulation of cytosolic substrate activity.[3] So long as $K_m \gg s$, hydrolytic rate rises in linear proportion to substrate activity. The signal therefore propagates through a volume distribution of enzyme decrementally and without distortion, with a characteristic space constant λ.[4] For a mean dark hydrolytic rate constant of 2.8 s^{-1} (Table II) with $D = 1.7 \times 10^{-7}$ cm^2 s^{-1}, $\lambda \approx 2.5$ μm. Thus changes in rod cGMP activity (from alteration of source or sink) propagate only a few micrometers, even in the dark. The importance of this restriction for signal dynamic range in the rod will be discussed under adaptation.

Dark-Active PDE

The identity of the dark-active PDE remains a puzzle. An upper bound on concentration, estimated from the kinetic constants of light-active PDE and the observed

[2] Assuming 1.6 nmol rhodopsin (mg protein)$^{-1}$ (Ames et al., 1986), 3 mM rhodopsin in the rod outer segments, and 0.5 vol fraction of cytoplasm. The discrepancy would diminish if only a fraction of rods in the isolated retina remained metabolically active, or if dark cGMP < 5 μM.

[3] Another perspective is that PDE is a diffusion-limited flux-optimized enzyme with $k_{cat}/K_m > 10^7$ s^{-1} M^{-1} (Stryer, 1988). In this instance Briggs-Haldane kinetics apply:

$$E + S \underset{k_1}{\overset{k_{-1}}{\leftrightarrow}} ES \xrightarrow{k_2} EP \leftrightarrow E + P;\ K_m = (k_{-1} + k_2)/k_1$$

Because the K_m for diffusion-limited enzymes reflects the value of k_2, the rate constant for the transition from *ES* to *EP*, catalytic efficiency demands a high value. Note that K_m is not an equilibrium constant for binding at the catalytic site.

[4] For constant isotropic PDE and GCy activity with the hydrolytic rate in linear proportion to substrate activity, steady-state cGMP diffusion reduces to to a one dimensional cable problem with space constant $\lambda_{cGMP} = \sqrt{D/R}$, where D is the diffusion constant and R the hydrolytic rate constant (Crank, 1956; Carslaw and Jaeger, 1965). Diffusional restriction reduces the value further, so the relation gives an upper bound.

dark T, is only 0.3 μM.[5] From this estimate dark active PDE represents $<1\%$ of the total light-activated enzyme, an amount nevertheless too large by a factor of 10^4 to attribute to excitation from thermal isomerization of rhodopsin along the established light-activated pathway (Baylor et al., 1980). If not from the ongoing isomerization of retinal, how does the dark PDE activity arise? A review of proposed mechanisms directs the search:

(*a*) Spontaneous dissociation of the inhibitory PDE_γ subunit: the equilibrium binding constant to $PDE_{\alpha\beta}$ ($K_{1/2} < 10$ pM, Wensel and Stryer, 1986, 1990) sets a lower limit on the concentration of catalytically active PDE*, even in the absence of G*. This amounts to activation of $<6 \times 10^{-4}$ total PDE, subject to the uncertainty of free PDE_γ in rods.

(*b*) Dark exchange of GTP onto G-GDP: whether this is negligible in vivo is a question; both opsin and incompletely phosphorylated forms of bleached rhodopsin promote exchange in vitro. The observation that rod current diminishes during GTPγS infusion into rods in darkness but is revived by IBMX supports this possibility, but has other interpretations as well (Lamb and Matthews, 1988*a*). In other receptor systems, the exchange rate in the absence of agonist is appreciable. Thus for the cardiac muscarinic potassium conductance, Breitwieser and Szabo (1988) estimate the limiting rate constant for the spontaneous GTPγS/GDP exchange in the absence of agonist at 0.44 min^{-1}. For rods with PDE* lifetime 0.9 s, this rate would correspond to activation of 6×10^{-3} PDE total.

(*c*) A distinct species of dark-active PDE: investigation has been limited by the difficulty of distinguishing native dark activity from an artifact of proteolytic attack on the gamma inhibitory subunit. Lipkin et al. (1988) described a fraction of rod PDE which could not be inhibited by added gamma subunit. Kawamura and Murakami (1986*a*) summarized evidence that the K_m is lower for dark active PDE. Gillespie et al. (1989) described a soluble form of PDE and with an uncertain relation to the transduction cascade.

From this short list, the need of in vivo investigations of GTP exchange onto G protein and of the action of PDE_γ in the dark is apparent. Finally, although the measured unbinding of cGMP at the noncatalytic sites on the PDE_β subunit seems much too slow for a regulatory role in the light response (off-rate $t_{1/2}$ 4 h in vitro, Gillespie and Beavo 1989), the possibility that binding in vivo differs sufficiently to admit a regulatory role in darkness should be kept in mind.

Light-Active PDE

In this work, the dependence of macroscopic PDE activity on isomerizations is linear without saturation over the physiologic range, in general agreement with Hodgkin and Nunn (1988). At issue is the relation between G* and PDE* in vivo.

[5] Estimates of K_m range from 130 μM dark PDE (Kawamura and Murakami, 1986*a*) to 1.3 mM light-activated (Barkdoll et al., 1988). Using K_m 130 μM, k_{cat} 2,000 s^{-1}, T 200 ms, gives a lower bound on the concentration of dark active enzyme,

$$E_D = \frac{K_m}{Tk_{cat}} = 0.3\ \mu M.$$

The linear relation might arise merely in the independence of G* domains excited by different photons, if these were too small to overlap. In salamander rods, independence with a flux of 10^5 isom s^{-1} and excited lifetime of 1 s requires that each R*→G*→PDE* domain occupy $< 1\text{-}\mu m^2$ disk membrane area. Measurements of the lateral diffusion coefficient of rhodopsin (0.5 μm^2 s^{-1}, Liebman et al., 1987) allow this possibility.

On the other hand, if photon domains of G* do overlap substantially then G* activation of PDE is constrained to be effectively linear. The stoichiometry of the G*–PDE interaction is disputed (Bennet and Clerc, 1989). The linearity of PDE activity in isomerizations found here remains consistent with the simplest assumption, that the interaction of PDE and G* is bimolecular. A pseudo-bimolecular relation might nevertheless be observed if the occupancy of some other G* binding site on PDE were nearly constant.

What controls the apparent decay rate of light-activated PDE*? From kinetic observations, this step might lie anywhere on the path from R* through PDE*. Proposed candidates are: (*a*) rhodopsin phosphorylation catalyzed by rhodopsin kinase; (*b*) suppression of R* or PDE* by arrestin (48-kD protein); (*c*) the GTP-ase activity of G*-GTP; (*d*) binding of the gamma inhibitory subunit to PDE*. The evidence reviewed here is inconclusive but defines the problem.

Schemes proposing a cooperative dependence of PDE activation on light or any dependence of quench rate on R* are not supported, because PDE* is linear in isomerizations and T_{PDE^*} is constant. Some hypotheses of the action of arrestin (48 kD) fall under this category (Zuckerman, 1986). Proposals of an accelerated deactivation of PDE* by cooperative interaction of PDE-gamma subunit released stoichiometrically from PDE on the binding of G_α-GTP encounter the same objection. Likewise schemes for an active regulatory role of Ca^{2+} in R* deactivation (Wagner et al., 1989) predict a variation of PDE activation with Ca^{2+} through light adaptation, not observed here.

Resolution of the rate control in vivo of R*, G*, and PDE* by nucleotide specificity has proved difficult. The rhodopsin kinase-mediated phosphorylation quench of R* requires $MgATP^{2-}$ and is not supported by GTP; the activation of α-transducin is specific to GTP. In truncated isolated rods supplied with guanine nucleotides only, the light response is prolonged, a phenomenon prevented by the addition of ATP to the perfusate (Yau and Nakatani, 1985). Intracellular perfusion with poorly hydrolyzed ATPγS prolongs intense flash responses, with delayed onset; AMP-PNP does not (Lamb and Matthews, 1988*b*), which may be explained merely by transfer of the terminal P-S to produce GTPγS (Otero et al., 1988).

The G_α GTP-ase reaction, the leading candidate for control of PDE deactivation, apparently does become rate limiting when GTP is replaced by the hydrolysis-resistant analogues GTPγS and GMP-PNP (Sather and Detwiler, 1987; Kondo and Miller, 1988; Lamb and Matthews, 1988*a*). Cells perfused internally with these molecules generate prolonged light responses to intense flashes. Such experiments support a requirement by PDE* deactivation for GTP hydrolysis but leave undefined the normal rate. Thus the question whether this step is fast and a preceding one normally rate-limiting remains open. The main objection to the GTPase hypothesis, the slowness of the rate in vitro, may be explained by the existence of different high

and low K_m forms or states of the G protein–associated GTPase (Sitaramayya et al. 1988).

Signal Dynamic Range and Adaptation

In the retina, rod membrane potential signals a $10^{+3.5}$-fold dynamic range of light intensity (Kleinschmidt and Dowling, 1975), but the excursion of PDE activity (as for metabolic flux) is only ~10-fold. Adaptation affecting the activation or deactivation of PDE seems not to be the mechanism of range compression. How can this discrepancy of scale be reconciled?

An important relation between PDE activation and rod signaling can be appreciated from considering the cGMP flux as a balance (Fig. 12). At steady state, cGMP

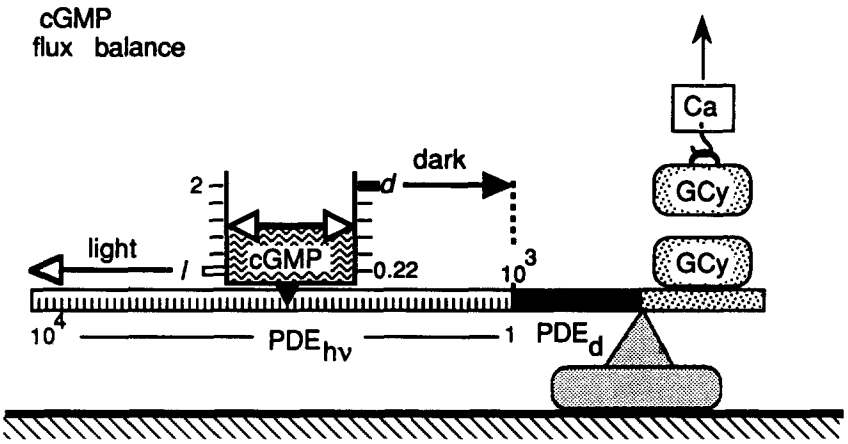

FIGURE 12. Signal dynamic range and the balance of cGMP flux. The model depicts the roles of light and dark active phosphodiesterase ($PDE_{h\nu}$ and PDE_d) in coupling the signal range of steady light intensity to a much smaller ratio of cGMP activity. The balance weighs rod cGMP flux; the rate of hydrolysis is proportional to the product of substrate and enzyme activities. The position of the pan along the beam is controlled by light-activated enzyme (calibrated in isomerizations s^{-1}); the height of cGMP in the pan is the messenger activity in μM (double arrow). The dark active PDE limits the height of the cGMP scale, *d*; the value at just saturating light intensity is denoted *l*. At equilibrium, the ratio *d*/*l* varies in proportion to $1 + PDE_{h\nu}/PDE_d$, see text eq. 25. Regulation of guanylyl cyclase (e.g., Ca^{2+}-mediated suppression) adjusts cGMP activity without altering the proportional relation of the PDE scale.

hydrolysis and synthesis are equal. The rate of cGMP hydrolysis is the product of PDE and cGMP activities (subscripts refer to light and dark active forms):

$$s(PDE_{h\nu} + PDE_d) = GCy \tag{25}$$

Consider the case in which GCy remains constant. If s_0 is cGMP activity in the dark ($PDE_{h\nu} = 0$), then $s_0/s = 1 + PDE_{h\nu}/PDE_d$. The proportional range of this linear scale, set by the magnitude of PDE_d, is ≈ 10:1, much less than the signal range of steady light intensity, ~3,000:1. The dark active PDE thus plays a significant role in scaling the modulation of substrate activity by the light-activated enzyme.

The dark-active PDE also scales the size of cGMP domains affected by individual isomerizations, through the space constant λ_{cGMP} (see above, subsection *Enzyme–Substrate Relations* and K_m). The PDE excited by an isomerization is probably associated to a single disk surface (Liebman et al., 1987), but single photon responses extend over a much larger portion of the rod, 3% in toad (Baylor et al., 1980), corresponding to 60 disks. Only the dark-active PDE affecting this domain is relevant to the local change of cGMP, not the gross total of the rod.[6] The scale relation affecting cGMP activity thus differs in the linear photon-counting regime from that observed in illumination bright enough to produce a spatially uniform current steady state.

The dark PDE contributes a scale relation in the time domain as well, through the time constant of cGMP hydrolysis. Feedback adjusts the balance of cGMP from the GCy source side, relieving saturation of the photocurrent, but also introduces the potential for instability. The transient cGMP activity signal produced by a light impulse depends substantially on a lag between input and feedback (Forti et al., 1989). In salamander rods the main time constants are $\approx$ 0.8 s for Ca efflux, $\approx$ 0.6 s for dark cGMP hydrolysis, and $\approx$ 0.9 s for light-activated PDE decay, so that all rates are about equally matched and the recovery of current after light stimulation can follow the Ca regulation of guanylyl cyclase or other sites without oscillation.

Finally, the linear range of PDE activation by steady light (with T_{PDE^*} constant) constrains the turnover of the G protein pool. In a steady light of isomerizing intensity B, linearity requires that only a minor fraction of the pool (denoted f) be exhausted by activation within the lifetime of G*. This relation constrains the number of copies of G* (denoted g) arising from an isomerization within the apparent lifetime of PDE*:

$$g < \frac{f\mathrm{G}}{BT_{PDE^*}} \tag{26}$$

The value found ($g < 170$) is plausible compared to biochemical measurements (Stryer, 1988).[7] Saturation of the light-sensitive current, on the other hand, occurs at light intensities insufficient to deplete the G pool appreciably and may be circumvented either by adaptive modulation of GCy or, possibly, of the cGMP-activated conductance (Filatov et al., 1989; Furman and Tanaka, 1989).

Conclusion

The rod outer segment is a model system for physiological and biochemical studies of cell messenger pathways. Biochemical descriptions have emphasized light-stimulated excitation; furthermore in rods no G protein mediating inhibition has been found. Signaling, however, depends critically on both the maintenance of a quiescent reference state and on a reset mechanism to restore this state after a stimulus (deactivation). This work defines the quiescent state of the rod cascade in terms of dark active PDE, and the apparent rates of light-stimulated PDE activation and

[6] Conditions do not reach steady state in the single photon response, so the scale of cGMP diffusion will be smaller than $\lambda_{cGMP} = \sqrt{D/R}$.

[7] For f = 0.3, G 300 μM, T 0.9 s, B 3 × 10^5 isom rod^{-1} s^{-1}, rod cytoplasm 10^{-12} l, $g \leq 170$.

deactivation. The relation of effector activation to the dynamic signal range of the rod may guide analysis of other G protein systems.

The rod achieves wide dynamic range mainly through a differential balance of cGMP flux (Fig. 12). The dual control of cGMP poised between a source and a sink introduces a degree of freedom independent of the signal amplitude, namely the absolute magnitude of enzyme activity. The dark-active PDE sets this value, establishing a ratio scale for the modulation of messenger by light active PDE. For intensities substantially above the single photon response range, the proportional range of this scale is ~10:1, much less than the signal range of steady light intensity, ≈ 3,000:1.

Definition of the proportional range of G protein activation by light awaits satisfactory measurement of the dark activity of G-GTP. The apparent lifetime of light-excited PDE (0.9 s) is constant through the signal range of both light and current. If this time reflects the rate of G-GTP hydrolysis, the constraint on turnover rate of the finite G-GDP pool may delimit the signal gain at the stage of G* activation.

Note added in proof: Following submission of this work in final form, two reports of Ca-binding regulatory protein affecting PDE and GCy appeared (Dizhoor et al., 1991; Kawamura and Murakami, 1991).

I thank Dr. Roy Furman for a gift of software, Drs. S. Ari, C. Blazynski, S. Kawamura, and J. Tanaka, and reviewers for criticism of the manuscript, and Professor P. Mueller for sponsorship.

This study was supported by grant EY0-6192 from the National Institutes of Health to Dr. Cobbs and grant EY0-1583 from the Vision Center to P. Liebman.

Original version received 16 January 1990 and accepted version received 30 January 1991.

REFERENCES

Ames, A., T. F. Walseth, R. A. Heyman, M. Barad, R. M. Graeff, and N. Goldberg. 1986. Light-induced increases in cGMP metabolic flux correspond with electrical responses of photoreceptors. *Journal of Biological Chemistry.* 261:13034–13042.

Applebury, M. L., and M. Chabre. 1986. Interaction of photoactivated rhodopsin with photoreceptor proteins: the cGMP cascade. *In* The Molecular Mechanism of Photoreception. H. Stieve, editor. Dahlem Konferenzen, Springer-Verlag, Berlin. 51–66.

Baehr, W., M. J. Devlin, and M. L. Applebury. 1979. Isolation and characterization of cGMP phosphodiesterase from bovine rod outer segments. *Journal of Biological Chemistry.* 254:11669–11677.

Barkdoll, A. E., E. N. Pugh, Jr., and A. Sitaramayya. 1988. Kinetics of the hydrolysis of 8-bromo-cyclic GMP by the light-activated phosphodiesterase of toad rods. *Journal of Neurochemistry.* 50:840–846.

Baylor, D. A., G. Matthews, and K.-W. Yau. 1980. Two components of electrical dark noise in toad rod outer segments. *Journal of Physiology.* 309:591–621.

Baylor, D. A., and B. Nunn. 1986. Electrical properties of the light-sensitive conductance of the salamander *Ambystoma tigrinum*. *Journal of Physiology.* 371:115–45.

Beavo, J. 1988. Multiple isozymes of cyclic nucleotide phosphodiesterase. *Advances in Second Messenger and Phosphoprotein Research.* 22:1–30.

Beavo, J. A., N. L. Rogers, O. B. Crofford, J. G. Hardman, E. W. Sutherland, and E. V. Newman. 1970. Effects of xanthine derivatives on lipolysis and adenosine 3′,5′-monophosphate phosphodiesterase activity. *Molecular Pharmacology.* 6:597–60.

Bennet, N. M., and A. Clerc. 1989. Activation of cGMP phosphodiesterase in retinal rods: mechanism of interaction with the GTP-binding protein (transducin). *Biochemistry.* 28:7418–7424.

Breitwieser, G. E., and G. Szabo. 1988. Mechanism of the muscarinic receptor-induced K^+ channel activation as revealed by hydrolysis-resistant GTP analogues. *Journal of General Physiology.* 91:469–493.

Brown, W. E., and A. V. Hill. 1923. The oxygen-dissociation curve of blood, and its thermodynamical basis. *Proceedings of the Royal Society Series B.* 94:297–334.

Carslaw, H. S., and J. C. Jaeger. 1959. Linear flow of heat in the rod. *In* Conduction of Heat in Solids. Clarendon Press, Oxford.

Cervetto, L., and P. A. McNaughton. 1986. The effects of phosphodiesterase inhibitors and lanthanum ions on the light-sensitive current of toad retinal rods. *Journal of Physiology.* 370:91–109.

Chabre, M., and P. Deterre. 1989. Molecular mechanism of visual transduction. Review. *European Journal of Biochemistry.* 179:255–266.

Cobbs, W. H. 1989. Light and dark active phosphodiesterase kinetic parameters probed by IBMX jumps: "cGMP clamp" in salamander rods. *Biophysical Journal.* 55:62*a*. (Abstr.)

Cobbs, W. H., and E. N. Pugh, Jr. 1985. Cyclic GMP can increase rod outer-segment light-sensitive current 10-fold without delay of excitation. *Nature.* 313:585–587.

Cobbs, W. H., and E. N. Pugh, Jr. 1987. Kinetics and components of the flash photocurrent of the larval salamander, Ambystoma tigrinum. *Journal of Physiology.* 394:529–572.

Crank, J. 1956. Simultaneous diffusion and chemical reaction. *In* The Mathematics of Diffusion. Clarendon Press, Oxford.

Dawis, S., R. M. Graeff, R. A. Heyman, T. F. Walseth, and N. D. Goldberg. 1988. Regulation of cyclic GMP metabolism in toad photoreceptors. *Journal of Biological Chemistry.* 263:8771–8785.

Dixon, M. 1953. The determination of enzyme inhibitor constants. *Biochemical Journal.* 55:170–171.

Dixon, H. B. F. 1982. Symbolism and terminology in enzyme reactions: recommendations of the Nomenclature Committee, International Union of Biochemistry. *European Journal of Biochemistry.* 128:281–291.

Dizhoor, A. M., S. Ray, S. Kumar, G. Niemi, M. Spencer, D. Brolly, K. A. Walsh, P. P. Philipov, J. B. Hurley, and L. Stryer. 1991. Recoverin: a calcium-sensitive activator of retinal rod guanylate cyclase. *Science.* 251:915–918.

Dratz, E. A., J. W. Lewis, L. E. Schaechter, and O. S. Kliger. 1987. Retinal rod GTPase turnover rate increases with concentration: a key in control of visual excitation? *Biochemical and Biophysical Research Communications.* 146:379–386.

Fersht, A. 1984. Enzyme-substrate complementarity and the use of binding energy in catalysis. *In* Enzyme Structure and Mechanism. 2nd edition. W. H. Freeman and Co., New York. 108.

Filatov, G. N., A. B. Jainazarov, S. S. Kolesnikov, A. L. Lyubarsky, and E. E. Fesenko. 1989. The effect of ATP, GTP, and cAMP on the cGMP-dependent conductance of the fragments from frog rod plasma membrane. *FEBS Letters.* 245:185–188.

Fleischman, D., and M. Denisevich. 1979. Guanylate cyclase of isolated bovine rod axonemes. *Biochemistry.* 18:5060–5066.

Forti, S., A. Menini, G. Rispoli, and V. Torre. 1989. Kinetics of phototransduction in retinal rods of the next *Triturus cristatus*. *Journal of Physiology.* 419:265–295.

Furman, R. E., and J. C. Tanaka. 1989. Photoreceptor channel activation: interaction between cyclic AMP and cyclic GMP. *Biochemistry.* 28:2785–2788.

Gillespie, P. G., and J. A. Beavo. 1989. cGMP is tightly bound to bovine retinal rod phosphodiesterase. *Proceedings of the National Academy of Sciences.* 86:4311–4315.

Gillespie, P. G., R. K. Prusti, E. Apel, and J. A. Beavo. 1989. A soluble form of bovine rod phosphodiesterase has a novel 15-kDa subunit. *Journal of Biological Chemistry.* 264:12187–12193.

Goldberg, N. D., A. Ames, J. E. Gander, and T. F. Walseth. 1983. Magnitude of increase in retinal cGMP metabolic flux determined by ^{18}O incorporation into nucleotide α-phosphoryls corresponds with intensity of photic stimulation. *Journal of Biological Chemistry.* 258:9213–9219.

Hodgkin, A. L., P. A. McNaughton, and B. J. Nunn. 1985. The ionic selectivity and calcium dependence of the light-sensitive current in rods. *Journal of Physiology.* 358:447–466.

Hodgkin, A. L., and B. J. Nunn. 1988. Control of light-sensitive current in salamander rods. *Journal of Physiology.* 403:439–471.

Kawamura, S., and M. Murakami. 1986*a*. Characterization of the light-induced increase in the Michaelis constant of the cGMP phosphodiesterase in frog rod outer segments. *Biochimica et Biophysica Acta.* 870:256–266.

Kawamura, S., and M. Murakami. 1986*b*. In situ cGMP phosphodiesterase and photoreceptor potential in Gecko retina. *Journal of General Physiology.* 87:737–759.

Kawamura, S., and M. Murakami. 1989. Regulation of cGMP levels by guanylate cyclase in truncated frog rod outer segments. *Journal of General Physiology.* 94:649–668.

Kawamura, S., and M. Murakami. 1991. Calcium-dependent regulation of cyclic GMP phosphodiesterase by a protein from frog retinal rods. *Nature.* 349:420–423.

Kleinschmidt, J., and J. Dowling. 1975. Intracellular recordings from gecko photoreceptors during light and dark adaptation. *Journal of General Physiology.* 66:617–648.

Koch, K.-W., and L. Stryer. 1988. Highly cooperative feedback control of retinal rod guanylate cyclase by calcium ions. *Nature.* 334:64–66.

Kondo, H., and W. H. Miller. 1988. Rod light adaptation may be mediated by acceleration of the phosphodiesterase-guanylate cyclase cycle. *Proceedings of the National Academy of Sciences, USA.* 85:1322–1326.

Lamb, T., and H. R. Matthews. 1988*a*. Incorporation of analogues of GTP and GDP into rod photoreceptors isolated from the tiger salamander. *Journal of Physiology.* 407:463–487.

Lamb, T., and H. R. Matthews. 1988*b*. Differential effects of the incorporation of ATP-analogues into rod photoreceptors isolated from the tiger salamander. *Journal of Physiology.* 401:94P.

Liebman, P. A., K. R. Parker, and E. A. Dratz. 1987. The molecular mechanism of visual excitation and its relation to the structure and composition of rod outer segment. *Annual Review of Physiology.* 49:765–91.

Lipkin, V. M., I. I. Dumler, K. G. Muradov, N. O. Artemyev, and R. N. Etingof. 1988. Active sites of the cGMP phosphodiesterase gamma-subunit of retinal rod outer segments. *FEBS Letters.* 234:287–290.

Matthews, H. R., R. L. Murphy, G. Fain, and T. Lamb. 1988. Photoreceptor light adaptation is mediated by cytoplasmic calcium concentration. *Nature.* 334:67–9.

Nakatani, K., and K-W. Yau. 1988*a*. Guanosine 3′,5′-cyclic monophosphate-activated conductance studied in a truncated rod outer segment of toad. *Journal of Physiology.* 395:731–53.

Nakatani, K., and K-W. Yau. 1988*b*. Calcium and light adaptation in retinal rods and cones. *Nature.* 334:69–71.

Nakatani, K., and K-W. Yau. 1988*c*. Calcium and magnesium fluxes across the plasma membrane of the toad rod outer segment. *Journal of Physiology.* 395:695–729.

Nichol, G. D., and M. D. Bownds. 1989. Calcium regulates some, but not all, aspects of light adaptation in rod photoreceptors. *Journal of General Physiology.* 94:233–259.

Otero, A., G. Breitwieser, and G. Szabo. 1988. Activation of muscarinic potassium currents by ATPγS in atrial cells. *Science* 242:443–445.

Pepe, I. M., A. Boero, L. Vergani, I. Panfoli, and C. Cugnoli. 1986. Effect of light and calcium on cyclic GMP synthesis in rod outer segments of toad retina. *Biochimica Biophysica Acta.* 889:271–6.

Pugh, E. N., Jr., and W. H. Cobbs. 1986. Visual transduction in vertebrate rods and cones: a tale of two transmitters. *Vision Research.* 26:1613–1643.

Reeves, M. L., B. K. Leigh, and P. J. England. 1987. The identification of a new cyclic nucleotide phosphodiesterase in human and guinea-pig cardiac ventricle. *Biochemical Journal.* 241:535–541.

Rispoli, G., and P. B. Detwiler. 1989. Light adaptation in Gecko rods may involve changes in both the initial and terminal stages of the transduction cascade. *Biophysical Journal.* 55:380*a*. (Abstr.)

Sather, W. A., and P. B. Detwiler. 1987. Intracellular biochemical manipulation of phototransduction in detached rod outer segments. *Proceedings of the National Academy of Sciences, USA.* 84:9290–9294.

Sitaramayya, A., C. Casadevall, N. Bennett, and S. Hakki. 1988. Contribution of the guanosine triphosphatase activity of G-protein to termination of light-activated guanosine cyclic 3,'5'-phosphate hydrolysis in retinal rod outer segments. *Biochemistry.* 27:4880.

Strinden, S. T., and R. H. Stellwagen. 1984. Inhibition of guanylate cyclases by methylxanthines and papaverine. *Biochemical and Biophysical Research Communications.* 123:1194–1200.

Stryer, L. 1988. Molecular basis of visual excitation. *Cold Spring Harbor Symposia in Quantitative Biology.* 53:283–294.

Torre, V., H. R. Matthews, and T. D. Lamb. 1986. Role of calcium in regulating the cGMP cascade of phototransduction in retinal rods. *Proceedings of the National Academy of Sciences, USA.* 83:7109–7113.

Vuong, T. M., and M. Chabre. 1990. Subsecond deactivation of transducin by endogenous GTP hydrolysis. *Nature.* 346:71–4.

Wagner R., N. Ryba, and R. Uhl. 1989. Calcium regulates the rate of rhodopsin disactivation and the primary amplification step in visual transuction. *FEBS Letters.* 242:249–254.

Wensel, T. G., and L. Stryer. 1986. Reciprocal control of retinal rod cyclic GMP phosphodiesterase by its gamma subunit and transducin. *Proteins.* 1:90–9.

Wensel, T. G., and L. Stryer. 1990. Activation mechanism of retinal rod cyclic GMP phosphodiesterase probed by fluorescein labeled inhibitory subunit. *Biochemistry.* 29:2155–61.

Williams, M., and M. Jarvis. 1988. Adenosine antagonists as potential therapeutic agents. *Pharmacology and Biochemistry of Behavior.* 29:433–31.

Yau, K.-W., and K. Nakatani. 1985. Light-suppressible, cGMP-sensitive conductance in the plasma membrane of a truncated rod outer segment. *Nature.* 317:252–255.

Zuckerman, R. 1986. A 48 kDa protein arrests cGMP phosphodiesterase activation in retinal rod disk membranes. *FEBS Letters.* 207:35–41.